Critical dynamics of stochastic models with energy conservation (model *C*)

R. Folk
Institute for Theoretical Physics, University of Linz, Linz, Austria

G. Moser
Institute for Physics and Biophysics, University of Salzburg, Salzburg, Austria

(Received 19 September 2003; published 4 March 2004)

We calculate the field-theoretic functions of the generalized dynamical model C^*, in which a conserved secondary density is coupled to a nonconserved complex order parameter, in two-loop order. We show that the fixed points in this extended model are equal to the fixed points obtained in model *C* with a real order parameter, which has been introduced by Halperin, Hohenberg, and Ma. Our results correct long-standing errors in the field-theoretic functions in model *C* published by several authors leading also to different fixed point values w^* for the ratio of the two time scales involved. The stability regions of the fixed points, which remained partially unclear, considered in a ''phase diagram''—whose axes are the spatial dimension d and number of order parameter components n—are now clarified. Especially an anomalous region found by previous authors, in which the scaling properties remained unsolved, does not exist. There are only two regions: one with a finite fixed point w^* where the dynamical exponent z of the order parameter is $z=2+\alpha/\nu$ and another region where $w^*=0$ and z is equal to the model *A* value.

DOI: 10.1103/PhysRevE.69.036101 PACS number(s): 05.70.Jk, 64.60.Ak, 64.60.Ht

I. INTRODUCTION

The dynamical critical behavior of a nonconserved order parameter (OP) may be described by the simple time-dependent Ginzburg-Landau model [1] (model *A*). However, the critical dynamics is determined by the slow modes and therefore conserved densities which couple to the OP have to be taken into account. In 1974 Halperin, Hohenberg, and Ma introduced such a model [2] in which a conserved secondary density (usually the energy density itself) is coupled to the nonconserved OP. The OP relaxes with the relaxation rate Γ and the conserved density diffuses with the diffusion rate λ.

This model has a wide spectrum of physical applications such as nonequilibrium relaxation [3], finite-size effects in the dynamics of the Ising model [4], systems with quenched impurities [5], and aging at criticality [6]. Physical realizations can be found in such different systems as intermetallic alloys [7], layers on solid substrates [8], and supercooled liquids [9].

Moreover, features relevant for models with energy conservation (model *C*) have been observed in another model describing the critical dynamics at a tricritical point [10]. Another interesting application of model *C* is found in the field of quantum chromodynamics describing the dynamics of quarks and gluons when one takes into account the baryon-number conservation law [11,12].

The theoretical analysis of model *C* by Halperin, Hohenberg, and Ma to first order in $\epsilon=4-d$ led to suggest various ''phase diagrams'' in the two-dimensional space whose axes are the spatial dimension d and number of the OP components, n. The ''phases'' in this space were characterized by the values of the stable fixed point for the time scale ratio $w=\Gamma/\lambda$ of the kinetic coefficients of the two dynamical densities. Three regions were found: region I with the fixed point $w^*=0$ (in one-loop order this is the region $n>4$), region II with $0<w^*=n/(2-n)<\infty$ (in one-loop order this is the region $n<2$), and the anomalous region III with $w^*=\infty$ (in one-loop order this is the region $2>n>4$). The one-loop order borderline value $n=4$ also separates the region with large n where $\alpha=0$ (α being the static exponent of the specific heat) from the region with small n where $\alpha>0$. In the first region the conserved density decouples from the OP in the asymptotics and need not to be taken into account for *asymptotic* critical properties. This is quite different in region II where the conserved density influences the dynamics of the OP in such away that both variables scale with the *same* exponent z but *different* from model *A*. Quite independent of the loop order in region II the value $z=2+\alpha/\nu$ (ν being the exponent of the correlation length) in the *anomalous* region the value of z and the validity of dynamical scaling behavior remained unclear. Model *C* was subsequently treated within the field-theoretical version of renormalization group theory up to two-loop order by Brezin and De Dominicis [13] and Murata [14].

The results of Brezin and De Dominicis in two-loop order corroborated a scenario where the anomalous region exists. They calculated the field-theoretic ζ and β functions which allow one to calculate the fixed points and corresponding critical exponents. However, the analysis was restricted to the ϵ-expansion technique. They obtained from their calculations at small values of ϵ boundary curves within region II separating region III from region II, although the extension of the anomalous region to the whole phase space could not be given. Further peculiarities—namely, a nonuniformity—appeared in the two-loop calculation when taking the limits $\epsilon\to 0$ and $w^*\to\infty$, which was believed to be the fixed-point value. A further subtlety appeared in region I, since the borderline for α changing sign and the fixed point $w^*=0$ being stable became different. This led to a small region I_a where the conserved density scales with $z_m=2+\alpha/\nu$ whereas the OP still scales with the dynamical critical exponent of model *A*. In the other region I, called I_b, the conserved density

decouples from the OP and its asymptotic critical dynamics is described by model *A*.

Subsequently Murata performed a second-order ϵ expansion and gave explicit results for the time ratio *w*. The fixed-point values contrary to exponents are dependent on the renormalization procedure and cannot be compared with the results of other methods. However, he recognized that in the anomalous region III, the fixed-point value of w^* showed an essential singularity and that this property might, even in the anomalous region, restore scaling and make the critical exponent take the value $z=2+\alpha/\nu$.

Halperin, Hohenberg, and Ma then compared their second- and higher-order results with results known at the time [15] and found agreement with the boundary curves of [13]. On the other hand, the peculiarities in the two-loop order and the results of [14] led them to the supposition that the anomalous region might not exist, but they were unable to draw a definite conclusion.

Recently we calculated the field-theoretic functions for a much more complicated model—for the dynamics of He^3-He^4 mixtures at the superfluid transition—containing the model *C* functions for $n=2$ as the limit of the properly reduced more complicated model [16]. Reducing our result for the field-theoretic functions to the simpler model *C* it turned out that our results differed from those of [13]. A calculation of the critical dynamics of model *C* for arbitrary *n* [17] then showed that the two-loop calculation of [13] was incorrect for all *n*. The correct result, however, allows us now to perform a systematic analysis of model *C* in two-loop order (a short account was given in [18]) by calculating the complete phase diagram and performing the limit to the one-loop results. This shows that no anomalous region III exists and that the standard systematic ϵ expansion breaks down for $2<n<4$. Previous results for the boundary curves at small ϵ were due to a mistaken application of the ϵ expansion, which cannot catch the essential singularity appearing in the fixed-point function $w^*(\epsilon,n)$. The boundary line previously found between regions I and II is correct. This was possible because the authors calculated the borderline by the equality of the dynamical critical exponents in the different regions.

In the following we reconsider model *C* starting from a generalization—model *C**—to a complex OP and in consequence from an OP dynamic equation with a complex relaxation rate Γ. This generalization is then for $n=2$ a limiting case of model *F* [19] without reversible terms. We then restrict our further study of the fixed-point properties to model *C* and calculate the fixed points, the stability exponents, and the flow of the dynamic parameters. A detailed comparison with the earlier field-theoretic results is then added. Several explicit calculations are collected in the Appendixes.

II. MODEL *C** EQUATIONS

Let us consider a system including a complex unconserved order parameter $\vec{\psi}_0(x,t)$ and a real conserved secondary density $m_0(x,t)$. The order parameter is assumed to be a vector with $n/2(n=2,4,...)$ components, while the secondary density should be a scalar quantity. In the absence of any mode coupling the critical dynamics of the order parameter is purely relaxational while the dynamics of the secondary density is determined by a diffusion process. This leads to the dynamic equations

$$\frac{\partial\vec{\psi}_0}{\partial t}=-2\mathring{\Gamma}\frac{\delta H}{\delta\vec{\psi}_0^\dagger}+\vec{\theta}_\psi, \tag{1}$$

$$\frac{\partial\vec{\psi}_0^\dagger}{\partial t}=-2\mathring{\Gamma}^\dagger\frac{\delta H}{\delta\vec{\psi}_0}+\vec{\theta}_\psi^\dagger, \tag{2}$$

$$\frac{\partial m_0}{\partial t}=\mathring{\lambda}_m\nabla^2\frac{\delta H}{\delta m_0}+\theta_m, \tag{3}$$

which we will call model C^* in the following. In the case of a real order parameter it reduces to model *C* [2]. The superscript † denotes complex-conjugated quantities. The kinetic coefficient of the order parameter $\mathring{\Gamma}=\mathring{\Gamma}'+i\mathring{\Gamma}''$ is also a complex quantity. The stochastic forces θ_{α_i} fulfill the relations

$$\langle\theta_{\psi_i}(x,t)\,\theta_{\psi_j}^\dagger(x',t')\rangle=4\mathring{\Gamma}'\,\delta(x-x')\,\delta(t-t')\,\delta_{ij}, \tag{4}$$

$$\langle\theta_m(x,t)\,\theta_m(x',t')\rangle=-2\mathring{\lambda}_m\nabla^2\delta(x-x')\,\delta(t-t'). \tag{5}$$

The critical behavior of the thermodynamic derivatives follows from the static functional

$$H=\int d^dx\left\{\frac{1}{2}\mathring{\tau}|\vec{\psi}_0|^2+\frac{1}{2}\sum_{i=1}^{n/2}\nabla\psi_{i0}\nabla\psi_{i0}^\dagger+\frac{\mathring{\tilde{u}}}{4!}|\vec{\psi}_0|^4+\frac{1}{2}a_m m_0^2+\frac{1}{2}\mathring{\gamma}_m m_0|\vec{\psi}_0|^2-\mathring{h}_m m_0\right\}, \tag{6}$$

with $|\vec{\psi}_0|^2\equiv\vec{\psi}_0\cdot\vec{\psi}_0^\dagger$. The centerdot denotes a $(n/2)$-dimensional scalar product. The above static functional may be reduced to the Ginzburg-Landau-Wilson functional with complex order parameter by integrating over the secondary density:

$$H_\psi=\int d^dx\left\{\frac{1}{2}\mathring{r}|\vec{\psi}_0|^2+\frac{1}{2}\sum_{i=1}^{n/2}\nabla\psi_{i0}\nabla\psi_{i0}^\dagger+\frac{\mathring{u}}{4!}|\vec{\psi}_0|^4\right\}. \tag{7}$$

The parameters *r* and *u* in Eq. (7) are related to τ, $\tilde{u}$, a_m, γ_m, and h_m in Eq. (6) by

$$\mathring{r}=\mathring{\tau}+\frac{1}{2}\frac{\mathring{\gamma}_m\mathring{h}_m}{a_m},\quad \mathring{u}=\mathring{\tilde{u}}-3\frac{\mathring{\gamma}_m^2}{a_m}. \tag{8}$$

The choice of an $(n/2)$-component order parameter in the equations above guarantees that the static functionals (6) and (7), and also all static properties derived from them, are fully equivalent to the corresponding static properties of a system with a real *n*-component order parameter. The ability to eliminate the secondary density in Eq. (6) also leads to a

relation between the correlations of the secondary density and order parameter correlations. For the first and second cumulants one obtains

$$\langle m_0(x)\rangle = \frac{1}{a_m}\left(\mathring{h}_m - \mathring{\gamma}_m\left\langle \frac{1}{2}|\vec{\psi}_0(x)|^2\right\rangle\right), \tag{9}$$

$$\langle m_0(x)m_0(0)\rangle_c = \frac{1}{a_m}\left(1+\frac{\mathring{\gamma}_m^2}{a_m}\left\langle \frac{1}{2}|\vec{\psi}_0(x)|^2\frac{1}{2}|\vec{\psi}_0(0)|^2\right\rangle_c\right). \tag{10}$$

Note that the angular brackets in Eqs. (9) and (10) have to be calculated with a probability density $\exp(-H)/\mathcal{N}$ on the left-hand side and with $\exp(-H_\psi)/\mathcal{N}'$ on the right-hand side, where $\mathcal{N}$ and $\mathcal{N}'$ are appropriate normalization factors. The static and dynamic vertex functions have to be calculated within the usual Feynman graph expansion. Details concerning the dynamic perturbation theory are given in Appendix A.

III. RENORMALIZATION OF MODEL *C**

Several renormalization schemes are available in the literature, which can be separated into two main classes. The first one uses ϵ expansion and the second one calculates all functions directly at $d=3$ where the theory is super renormalizable [20]. The second class makes it necessary to identify and sum up the contributions of the T_c shift and the correlation length carefully in all functions in order to avoid singularities at $d=3$, while in the first class it is necessary to collect singularities at $d=4$ in renormalization factors. This can be done in several ways like using normalization conditions or performing a minimal subtraction in which the pole terms only are collected (for an overview see [21]). Also a renormalization scheme which uses methods of both classes has been developed [22] where the renormalization factors are determined by using the ϵ expansion with the minimal subtraction scheme, while the finite amplitudes are calculated at $d=3$.

Because renormalization of model *C* is known in principle [13], we have shifted the explicit introduction of *Z* factors into Appendix B. There we have defined all *Z* factors in order to clarify the notation we will use. We want to emphasize that our introduction of renormalized parameters is not restricted to a specific renormalization scheme.

A. ζ functions

The ζ functions following from the renormalization factors introduced in Appendix B are not uniquely defined so that they are differently introduced in the literature depending on the authors. We will use in statics and dynamics the definition [23]

$$\zeta_{a_i}(\{a_j\}) = \frac{d\ln Z_{a_i}^{-1}}{d\ln\kappa} \tag{11}$$

in the following, where $\{\alpha_j\}=\{u,\gamma,\Gamma,\Gamma^\dagger,\lambda\}$ is the set of static and dynamic model parameters. a_i stands for any density ψ, m, $\tilde{\psi}$, $\tilde{m}$ or any model parameter α_i. The only exception in the definition of the ζ functions is the additive renormalization A_{ψ^2} of the specific heat introduced in Eq. (B9), which leads to

$$B_{\psi^2}(u) = \kappa^\epsilon Z_{\psi^2}^2 \kappa \frac{d}{d\kappa}(Z_{\psi^2}^{-2}\kappa^{-\epsilon}A_{\psi^2}). \tag{12}$$

The relations (B7) and (B9) between the static *Z* factors mentioned in Appendix B lead also to relations between the ζ functions, which are

$$\zeta_\gamma(u,\gamma) = 2\zeta_m(u,\gamma)+\zeta_\psi(u)+\zeta_{\psi^2}(u) \tag{13}$$

and

$$\zeta_m(u,\gamma) = \frac{1}{2}\gamma^2 B_{\psi^2}(u), \tag{14}$$

respectively. The second relation can be used to eliminate ζ_m in the first one. Thus we obtain

$$\zeta_\gamma(u,\lambda) = \gamma^2 B_{\psi^2}(u)+\zeta_\psi(u)+\zeta_{\psi^2}(u), \tag{15}$$

where all functions on the right-hand side are determined by the Ginzburg-Landau-Wilson model (7). The ζ functions of the kinetic coefficients Γ, $\Gamma^\dagger$, and λ follow from the *Z*-factor relation (B15) by inserting them into Eq. (11). We obtain

$$\zeta_\Gamma(u,\gamma,\Gamma,\Gamma^\dagger,\gamma) = -\frac{1}{2}\zeta_{\tilde{\psi}^\dagger}(u,\gamma,\Gamma,\Gamma^\dagger,\lambda)+\frac{1}{2}\zeta_\psi(u), \tag{16}$$

$$\zeta_{\Gamma^\dagger}(u,\gamma,\Gamma,\Gamma^\dagger,\lambda) = \zeta_\Gamma^\dagger(u,\gamma,\Gamma,\Gamma^\dagger,\lambda), \tag{17}$$

$$\zeta_\lambda(u,\gamma) = 2\zeta_m(u,\gamma). \tag{18}$$

With Eq. (14) we obtain for the third equation

$$\zeta_\lambda(u,\gamma) = \gamma^2 B_{\psi^2}(u). \tag{19}$$

In order to obtain fixed points within dynamics the complex time scale ratio

$$w = \frac{\Gamma}{\lambda} \tag{20}$$

is usually introduced. Inserting Eqs. (16)–(19) into $\zeta_w=\zeta_\Gamma-\zeta_\lambda$ we see immediately that the ζ function of the time scale ratio w is

$$\zeta_w(u,\gamma,w,w^\dagger) = \frac{1}{2}\zeta_\psi(u)-\frac{1}{2}\zeta_{\tilde{\psi}^\dagger}(u,\gamma,w,w^\dagger)-\gamma^2 B_{\psi^2}(u). \tag{21}$$

The ζ function of $w^\dagger$ is the complex conjugate of Eq. (21).

B. β functions

The β functions for static or dynamic model parameters α_i are generally defined as

$$\beta_{\alpha_i}(\{\alpha_j\}) = \alpha_i[-c_i+\zeta_{\alpha_i}(\{\alpha_j\})], \tag{22}$$

where c_i is the cutoff dimension of the corresponding parameter. For the static couplings u and γ the cutoff dimensions c have the values ϵ and $\epsilon/2$, respectively. All kinetic coefficients Γ, $\Gamma^\dagger$, and λ are dimensionless quantities regarding the cutoff dimension, which means $c=0$. Equation (B8) leads to the static β function

$$\beta_\gamma(u,\gamma)=\gamma\left(-\frac{\epsilon}{2}-\zeta_\psi(u)-\zeta_m(u,\gamma)+\zeta_\gamma(u,\gamma)\right). \quad (23)$$

The β function of the time scale ratio w can be written as

$$\beta_w(u,\gamma,w,w^\dagger)=w\zeta_w(u,\gamma,w,w^\dagger), \quad (24)$$

which follows immediately from Eq. (22). Since the cutoff dimension c_i of all kinetic coefficients is zero, it is zero also for ratio w; see Eq. (20). The flow equations of the three relevant model parameters are explicitly given by

$$l\frac{du}{dl}=\beta_u(u), \quad (25)$$

$$l\frac{d\gamma}{dl}=\beta_\gamma(u,\gamma), \quad (26)$$

$$l\frac{dw}{dl}=\beta_w(u,\gamma,w,w^\dagger). \quad (27)$$

The complex equation (27) includes two separate differential equations, one for the real part w' and one for imaginary part w'':

$$l\frac{dw'}{dl}=\beta'_w(u,\gamma,w,w^\dagger), \quad (28)$$

$$l\frac{dw''}{dl}=\beta''_w(u,\gamma,w,w^\dagger). \quad (29)$$

Each of the β functions above is expressed by certain ζ functions according to its definition and the relations in Appendix B. Equation (B2) leads immediately to the expression

$$\beta_u(u)=u[-\epsilon-2\zeta_\psi(u)+\zeta_u(u)]. \quad (30)$$

Using the relations between the ζ functions given in Eqs. (13)–(21) we obtain for model C^* the following β functions for γ and w:

$$\beta_\gamma(u,\gamma)=\gamma\left(-\frac{\epsilon}{2}+\zeta_{\psi^2}(u)+\frac{1}{2}\gamma^2 B_{\psi^2}(u)\right), \quad (31)$$

$$\beta_w(u,\gamma,w,w^\dagger)=w\left(\frac{1}{2}\zeta_\psi(u)-\frac{1}{2}\zeta_{\tilde\psi^\dagger}(u,\gamma,w,w^\dagger)-\gamma^2 B_{\psi^2}(u)\right). \quad (32)$$

Only one complex dynamic ζ function—$\zeta_{\tilde\psi^\dagger}$—appears in the above equations and has to be determined from dynamic perturbation expansion. All other functions are known from the Ginzburg-Landau-Wilson model (7).

C. Two-loop results

The static ζ functions of the Ginzburg-Landau-Wilson model (7) are well known up to two-loop order and in higher-loop order within several renormalization approaches. We will restrict ourself to the minimal subtraction scheme in the following. The static ζ functions in this approach in two-loop order are

$$\zeta_\psi(u)=-\frac{n+2}{72}u^2, \quad (33)$$

$$\zeta_u(u)=\frac{n+8}{6}u-\frac{5n+22}{18}u^2, \quad (34)$$

$$\zeta_{\psi^2}(u)=\frac{n+2}{6}u\left(1-\frac{5}{12}u\right), \quad (35)$$

$$B_{\psi^2}(u)=\frac{n}{2}. \quad (36)$$

Two-loop expressions for the dynamic function $\zeta_{\tilde\psi^\dagger}$ or ζ_Γ, respectively, have been calculated by several authors so far only for the real model C (real order parameter $\psi=\psi^\dagger\equiv\phi$ and real kinetic coefficient $\Gamma=\Gamma^\dagger$). Two results for the dynamic ζ functions have been published [13,19] (the second reference treats only the special case $n=2$); a third calculation has remained unpublished [24]. All of them obtained different results for the ζ_Γ function. Although it remained unclear which result is the correct one, some comments could have been made. (i) The result for ζ_Γ of [13] contains some very strange properties even for $\epsilon=1$ (see Chap. VI). (ii) The result of [19] did not reduce to model A in the limit where the ratio of the time scales w goes to zero and the static coupling γ stays finite.

An answer to this open problem can only be given by an independent calculation. Our calculation uses structures in the perturbative expressions [16] which allow a separation of static and dynamic contributions before the renormalization is performed. Since the correlation length remains unrenormalized, a perturbational resummation of the correlation length leads to expressions which are easy to survey. Finaly only five independent integrals remain whose poles determine the renormalization factors. The structure of the perturbation theory also give rise to specific relations of various vertex functions and allows internal consistency checks of the expressions. Details are given in Appendix A 2. From our two-loop calculation we obtain the dynamic ζ function in the complex model C^*:

$$\zeta_{\tilde{\psi}^\dagger}(u,\gamma,w,w^\dagger) = -2\frac{w\gamma^2}{1+w} + \frac{w\gamma^2}{1+w}\left[\frac{n+2}{3}u(1-L_0-x_1L_1) + \frac{w\gamma^2}{1+w}\left(\frac{n}{2} - \frac{w}{1+w} - \frac{n+2}{2}(L_0+x_1L_1) - \frac{1+2w}{1+w}\ln\frac{(1+w)^2}{1+2w}\right)\right] - \frac{n+2}{18}u^2\left(L_0+x_1L_1-\frac{1}{4}\right), \quad (37)$$

where the following notation has been introduced:

$$x_1 = 2 + \frac{w}{w^\dagger}, \quad (38)$$

$$L_0 = 2\ln\frac{2}{1+\frac{w^\dagger}{w}}, \quad L_1 = \ln\frac{\left(1+\frac{w^\dagger}{w}\right)^2}{1+2\frac{w^\dagger}{w}}. \quad (39)$$

The ζ function ζ_Γ in Eq. (16), which corresponds to the kinetic coefficient, is given by

$$\zeta_\Gamma(u,\gamma,w,w^\dagger) = \frac{w\gamma^2}{1+w} - \frac{1}{2}\frac{w\gamma^2}{1+w}\left[\frac{n+2}{3}u(1-L_0-x_1L_1) + \frac{w\gamma^2}{1+w}\left(\frac{n}{2} - \frac{w}{1+w} - \frac{n+2}{2}(L_0+x_1L_1) - \frac{1+2w}{1+w}\ln\frac{(1+w)^2}{1+2w}\right)\right] + \frac{n+2}{36}u^2\left(L_0+x_1L_1-\frac{1}{2}\right). \quad (40)$$

In the case of the real model C ($w=w^\dagger$) the expression $L_0 + x_1L_1$ reduces to $L=3\ln 4/3$ in Eqs. (40) and (37) and ζ_Γ is then in agreement with [24].

IV. FIXED POINTS AND STABILITY

A. Fixed points

1. Static fixed points

The fixed points of β functions which are based on static functionals of the type (6) or (7) are well known. Hence it is sufficient to give a short survey. The fixed points u^* and γ^* of the static couplings are determined by the conditions

$$\beta_u(u^*)=0, \quad \beta_\gamma(u^*,\gamma^*)=0, \quad (41)$$

independent of the model type because both the complex model C^* and the real model C use the same static functional.

The fixed point values of the fourth-order coupling u are well known from the ϕ^4 model. They are (i) the Gaussian fixed point $u^*=0$ and (ii) the Heisenberg fixed-point value $u^*=u_H$, which reads ϵ expanded in two-loop order

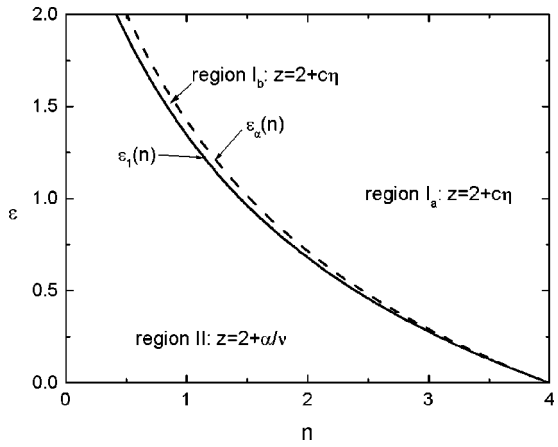

FIG. 1. Regions of existence of different fixed points: $\epsilon_\alpha(n)$ separates the region with nondiverging ($\gamma^*\equiv 0$, right side) from those with diverging ($\gamma^*\neq 0$, left side) specific heat (dashed curve). The solid curve $\epsilon_1(n)$ separates the region where the fixed point $\rho^*(\epsilon,n)\equiv 0$ is stable (right side) from those where it is unstable (left side).

$$u_H = \frac{6\epsilon}{n+8}\left(1+\frac{3(3n+14)}{(n+8)^2}\epsilon\right). \quad (42)$$

Independent of the value for the fixed point of u, $\gamma^*=0$ is a fixed point for the coupling γ as the second equation in Eqs. (41) shows. There exist also nontrivial fixed points γ^* depending on the fixed-point values of u. From the β function (31) one can see that the equation $\beta_\gamma(u^*,\gamma^*)=0$ has the following solutions

(i) In the case $u^*=0$ one obtains

$$\gamma^{*2} = \gamma_O^2 = \frac{2\epsilon}{n}. \quad (43)$$

(ii) In the case of $u^*=u_H$ one has

$$\gamma^{*2} = \gamma_C^2 = \frac{\alpha}{\nu B_{\psi^2}(u^*)}, \quad (44)$$

where use has been made of the identification of the specific heat exponent α by the ζ function ζ_{ψ^2}. Both expressions are valid in all orders of perturbation expansion. The ϵ-expanded expression of Eq. (44) reads in two-loop order

$$\gamma_C^2 = \frac{2\epsilon}{n(n+8)}\left(4-n-\frac{(n+2)(13n+44)}{(n+8)^2}\epsilon\right). \quad (45)$$

Considering the ϵ-expanded expression for γ_C^2 in the whole ϵ-n plane it turns out that there is a region in which γ_C^2 is negative and therefore no real fixed-point value for γ exists. The boundary of existence, $\epsilon_\alpha(n)$, of a real fixed-point value for γ is determined by $\gamma_C^2(\epsilon,n)=0$ (corresponding to $\alpha=0$) and is drawn as a dashed line in Fig. 1.

2. Dynamic fixed points

The dynamic fixed points are determined by the zeros of the β function of w, which leads to the two coupled conditions

$$\beta_w'(u^*,\gamma^*,w^*,w^{\dagger *})=0, \quad \beta_w''(u^*,\gamma^*,w^*,w^{\dagger *})=0, \tag{46}$$

in the complex case, and to the single equation

$$\beta_w(u^*,\gamma^*,w^*)=0, \tag{47}$$

in the real case. The static fixed points determine the allowed dynamic fixed points when inserted into Eqs. (46) or (47). An examination of the two equations in Eqs. (46) reveals that no additional fixed points with nonvanishing imaginary part appear in model C^*, which means that we have for all fixed points

$$w''^*=0. \tag{48}$$

Thus Eqs. (46) reduce to Eq. (47) at the fixed points and their discussion can be restricted to model C in the following.

In order to simplify the following discussion of the fixed points in the real model C it is more appropriate to change from the time scale ratio w to the parameter

$$\rho=\frac{w}{1+w}. \tag{49}$$

This transformation maps the infinite range 0 to ∞ of w to the finite region ranging from 0 to 1 ($w=\infty$ corresponds to $\rho=1$). The function $\zeta_w(u,\gamma,w)$ in Eq. (40) can be rewritten as a function $\zeta_w(u,\gamma,\rho)$:

$$\zeta_w(u,\gamma,\rho)=\left(\rho-\frac{n}{2}\right)\gamma^2-\frac{1}{2}\rho\gamma^2\left[\frac{n+2}{3}u(1-L)+\rho\gamma^2\left(\frac{n}{2}-\rho-\frac{n+2}{2}L+(1+\rho)\ln(1-\rho^2)\right)\right]+\frac{n+2}{36}u^2\left(L-\frac{1}{2}\right). \tag{50}$$

The flow equation for ρ,

$$l\frac{d\rho}{dl}=\beta_\rho(u,\gamma,\rho), \tag{51}$$

follows from Eq. (22). From the definition (49) and (27) we obtain the β function

$$\beta_\rho(u,\gamma,\rho)=\rho(1-\rho)\zeta_w(u,\gamma,\rho), \tag{52}$$

with ζ_w given in Eq. (50). A survey over the fixed points in model C^*/C is given in Table I. For convenience we have listed not only the fixed-point values of ρ, but also the corresponding values of the time scale ratio w (last column) in Table I.

At each static fixed point defined by u^* and γ^* except the Gaussian fixed point, the β function (52) basically implies three types of dynamic fixed points: namely, $\rho^*=0$, $\rho^*=1$, and a fixed-point value $\rho^*=\rho_C$ resulting from the equation $\zeta_w(u^*,\gamma^*,\rho_C)=0$.

TABLE I. Fixed points of model C.

u^*	γ^*	ρ^*	w^*
0	0	$0\leqslant\rho^*\leqslant 1$	$0\leqslant w^*\leqslant\infty$
	γ_O	0	0
		ρ_O	w_O
		1	∞
u_H	0	0	0
		1	∞
	γ_C	0	0
		ρ_C	w_C
		1	∞

At the Gaussian fixed point ($u^*=0,\gamma^*=0$), ζ_w vanishes independent of the value of ρ and thus each fixed-point value between 0 and 1 is allowed; see Table I. Because ζ_w is a power series in u and γ, this is true in all orders of perturbation expansion.

In the case $u^*=u_H$, $\gamma^*=0$ a special situation occurs because the possible values of ρ^* depend on the order of perturbation theory. In two-loop order ζ_w in Eq. (50) is always different from zero due to the u^2 contribution of model A. Thus only two corresponding fixed points $\rho^*=0$ and $\rho^*=1$ are allowed, which is also valid in all higher orders of perturbation expansion. The structure outlined in Table I is valid in two-loop order. In one-loop order these two ρ fixed points degenerate to a line of fixed points ranging from 0 to 1. The reason is that ζ_w is proportional to γ^2 and no u terms appear in one-loop order. In the case $\gamma^*=0$ the one-loop function $\zeta_w(u^*,\gamma^*,\rho^*)$ is zero, independent of the value of ρ^*.

In order to obtain the solutions ρ^* from the nonlinear equation $\zeta_w(u^*,\gamma^*,\rho^*)=0$ we have two ways to proceed. The first one is to use strictly the ϵ expansion up to the second order and the second one is to look numerically for solutions ρ^* of the nonlinear equation.

Inserting the static fixed-point values of u and γ from Eqs. (42)–(45) up to order ϵ^2 into $\zeta_w(u^*,\gamma^*,\rho^*)=0$ (note that ζ_w is then proportional to ϵ) and performing the ϵ expansion consequently, we obtain the ϵ-expanded fixed-point values of ρ for two different values of the u^* (see Table I). In the case of $u^*=0$,

$$\rho_O=\frac{n}{2}\left\{1+\frac{\epsilon}{2}\left[\left(1+\frac{n}{2}\right)\ln\left(1-\frac{n^2}{4}\right)-\frac{n+2}{2}L\right]\right\}. \tag{53}$$

In the case of the Heisenberg fixed point $u^*=u_H$,

$$\rho_C=\frac{n}{2}\{1+b_c\epsilon\}, \tag{54}$$

$$b_c=\frac{(n+2)}{(n+8)}\left[1-\frac{8-n}{4}L+\frac{4-n}{4}\ln\left(1-\frac{n^2}{4}\right)-\frac{1}{(4-n)}\left(L-\frac{1}{2}\right)\right]. \tag{55}$$

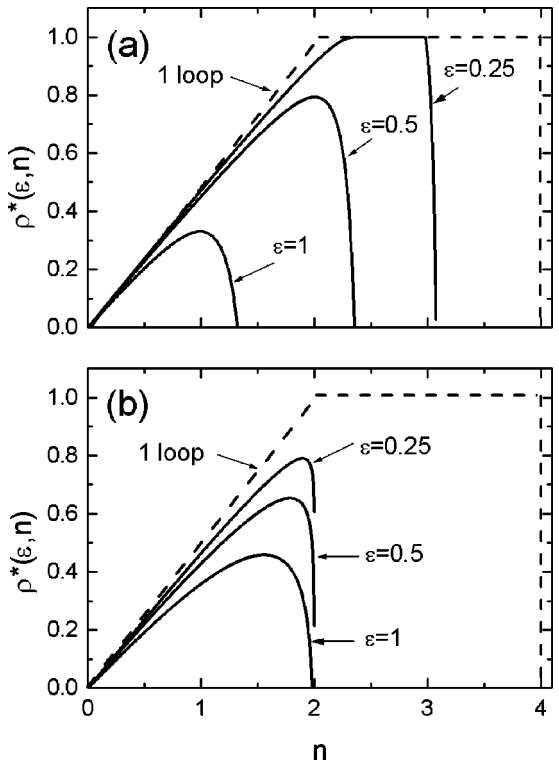

FIG. 2. Fixed point for $\rho=w/(1+w)$ as a function of the order parameter dimension n for several space dimensions d ($\epsilon=4-d$). (a) Results of the nonlinear solution of Eq. (47) and (b) results of the ϵ expansion. The one-loop order has not changed the region of existence of the fixed point contrary to case (a). The one-loop fixed points are plotted as dashed lines in both figures.

One can see that obviously in any dimension the existence borderline lies at $n=2$. This is caused by the logarithmic terms in two-loop order. The finite fixed point $0<\rho_C<1$ only exists for $n<2$; otherwise, the logarithms have negative arguments. This type of logarithmic term is not restricted to the second order of perturbation expansion but also appears in higher-order contributions, restricting the existence of the ϵ-expanded solution always to $0\leqslant n<2$. Thus it seems to be an artifact of the ϵ expansion, indicating that it is a less suitable method to treat fixed points of time scale ratios in model *C*. In [13] the authors tried to overcome this borderline by inserting the ϵ expansion iteratively, in a nonsystematic way.

Instead we calculate the fixed points of ρ by solving Eq. (47) directly [25], avoiding the artificial existence boundary at $n=2$. This procedure is valid in our opinion since ρ and w, respectively, is not a coupling and appears in the β function in a nonpolynomial way. In order to illustrate this we have plotted in Fig. 2 the fixed-point values ρ_C as a function of n at different dimensions $\epsilon=1$ ($d=3$), $\epsilon=0.5$, and $\epsilon=0.25$. In Fig. 2(a) the nonlinear solution is drawn while in Fig. 2(b) the corresponding results of the ϵ expansion (54) is given.

As can be seen from Fig. 2(a) a new borderline appears as a function of ϵ where the nonzero solution, which has to be positive, goes to zero at finite nonzero n. This defines the *existence* borderline $\epsilon_1(n)$ (see Fig. 1) given by the equation

$$\zeta_w(u_H,\gamma_C,\rho=0)=0. \tag{56}$$

This reads explicitly to all orders

$$c\,\eta-\frac{\alpha}{\nu}=0, \tag{57}$$

where we have used $[\zeta_\psi(u)-\zeta_{\bar{\psi}^\dagger}(u,0,\rho)]/2=\zeta_\Gamma^{(A)}(u_H)\equiv c\,\eta$, Eqs. (19) and (44).

In Fig. 2(a) the nonlinear solution for the fixed point at $\epsilon=0.25$ appears to reach the value 1 (equivalent to $w^*=\infty$) but actually this is not the case. In contrast, the dashed one-loop solution does have the value 1 in the considered region. The fixed-point value remains below 1 but stays so close to it that it cannot be resolved in the figure. This can be verified by examining ζ_ρ very close at $\rho=1$. Expanding the fixed-point value ρ^* about 1, the leading terms $\rho_{as}^*(\epsilon,n)$ read

$$\rho_{as}^*(\epsilon,n)=1-0.5\exp[-a(\epsilon/n)/\gamma^{*2}]\equiv 1-x, \tag{58}$$

with

$$a(\epsilon,n)=\frac{n}{2}-1+\frac{n+2}{6}u^*(1-L)+\frac{\gamma^{*2}}{2}\left(\frac{n}{2}-1-\frac{n+2}{2}L\right)$$
$$-\frac{(n+2)u^{*2}}{36\gamma^{*2}}\left(L-\frac{1}{2}\right) \tag{59}$$

proving to be smaller than 1. Thus there is no anomalous region where the fixed-point value is 1. Therefore the dynamical critical exponent is in all orders of perturbation theory $z=2+\alpha/\nu$ [this is easily derived from Eq. (21); see [13]].

One also sees in Fig. 2(a) that the nonlinear solution for the fixed point reaches in the limit $\epsilon\to 0$ the one-loop solution in the region $0\leqslant n\leqslant 4$. The ϵ-expanded solution in Fig. 2(b) reaches the one-loop fixed-point values only in the region $0\leqslant n<2$.

B. Stability of the fixed points

A fixed point is considered stable when an arbitrary small deviation of the initial values of the flow equations from the fixed point values leads to a flow which runs into the fixed point again. Linearizing the flow equations (25)–(27) around the fixed-point value one can introduce the transient exponents as the eigenvalues of the matrix

$$\left[\frac{\partial\beta_j}{\partial\alpha_i}\right]=\begin{pmatrix} \frac{\partial\beta_u}{\partial u} & \frac{\partial\beta_\gamma}{\partial u} & \frac{\partial\beta_w}{\partial u} & \frac{\partial\beta_{w^\dagger}}{\partial u} \\ 0 & \frac{\partial\beta_\gamma}{\partial\gamma} & \frac{\partial\beta_w}{\partial\gamma} & \frac{\partial\beta_{w^\dagger}}{\partial\gamma} \\ 0 & 0 & \frac{\partial\beta_w}{\partial w} & \frac{\partial\beta_{w^\dagger}}{\partial w} \\ 0 & 0 & \frac{\partial\beta_w}{\partial w^\dagger} & \frac{\partial\beta_{w^\dagger}}{\partial w^\dagger} \end{pmatrix}. \tag{60}$$

From the structure of Eq. (60) we can see that the derivatives of the static β functions decouple from the dynamic derivatives. Thus we obtain the static eigenvalues

$$\lambda_u = \frac{\partial \beta_u}{\partial u}, \quad \lambda_\gamma = \frac{\partial \beta_\gamma}{\partial \gamma}. \tag{61}$$

The complex time scale ratio and its complex conjugated form a two-dimensional subspace with eigenvalues

$$\lambda_\pm = \frac{1}{2}\left\{ \frac{\partial \beta_w}{\partial w} + \frac{\partial \beta_{w^\dagger}}{\partial w^\dagger} \pm \sqrt{\left(\frac{\partial \beta_w}{\partial w} - \frac{\partial \beta_{w^\dagger}}{\partial w^\dagger} \right)^2 + 4 \frac{\partial \beta_w}{\partial w^\dagger} \frac{\partial \beta_{w^\dagger}}{\partial w}} \right\}. \tag{62}$$

In the case of the real model C the above eigenvalues (62) reduce to

$$\lambda_+ \equiv \lambda_w = \frac{\partial \beta_w}{\partial w}, \quad \lambda_- = 0. \tag{63}$$

The transient exponents for a given fixed point are defined as the eigenvalues taken at the corresponding fixed-point values $\{\alpha_i^*\}$ of the parameters. Since for model C, λ_- is zero, in any case this means that a nonzero initial value of the imaginary part of w decays very slowly (in fact logarithmically; see Sec. V).

1. Stability of the static fixed points

The following considerations are valid for both the complex and real modes. The static transient exponents are

$$\omega_u \equiv \left. \frac{\partial \beta_u}{\partial u} \right|_{\{\alpha_i\} = \{\alpha_i^*\}}, \tag{64}$$

$$\omega_\gamma \equiv \left. \frac{\partial \beta_\gamma}{\partial \gamma} \right|_{\{\alpha_i\} = \{\alpha_i^*\}}. \tag{65}$$

The two transient exponents define the stability of the static fixed points. The conditions

$$\omega_u > 0, \quad \omega_\gamma > 0 \tag{66}$$

define a region in the space dimension and order parameter component (ϵ-n) plane in which the considered static fixed point is stable. Of all static fixed points listed in Table 1 only those which fulfill Eq. (66) are stable and therefore determine the critical behavior for certain order parameter components n and spatial dimensions d. The static fixed points are well known and will be briefly discussed. Within the Ginzburg-Landau-Wilson model the transient exponents are

$$u^* = 0 \Rightarrow \omega_u = -\epsilon, \tag{67}$$

$$u^* = u_H \Rightarrow \omega_u = \epsilon \left(1 - \frac{3(3n+14)}{(n+8)^2} \epsilon \right). \tag{68}$$

Thus in $d=3$ the Heisenberg fixed point u_H is the stable one because ω_u in Eq. (68) is positive for all values of n. We only need to consider the γ and w fixed points which correspond to u_H. According to Fig. 1 two γ fixed points exist. Calculating the transient exponents from β_γ we obtain

$$\gamma^* = 0 \Rightarrow \omega_\gamma = \omega_c, \tag{69}$$

$$\gamma^* = \gamma_C \Rightarrow \omega_\gamma = -\omega_c. \tag{70}$$

The ϵ-expanded transient exponent ω_c reads in second order

$$\omega_c = \frac{\epsilon}{2(n+8)} \left(n - 4 + \frac{(n+2)(13n+44)}{(n+8)^2} \epsilon \right). \tag{71}$$

The stability of the two γ fixed points depends on the sign of ω_c, which itself is dependent on the value of n. The condition is now that the expression in the bracket in Eq. (71) has to be positive.

Considering only the first order (one loop) in the perturbation expansion we see that the boundary of stability would be $n=4$. For $n>4$ we would have $\omega_c > 0$ which means that for this case the fixed point $\gamma^*=0$ would be stable and that in the case $n<4$ the fixed point $\gamma^* = \gamma_c$ would be the stable one. The second-order (two-loop) perturbation expansion adds a positive contribution (order-ϵ terms) to the expression in the brackets shifting the boundary to lower values of n. The boundary is now determined by the equation $n^3 + 25n^2 + 70n - 168 = 0$ (at $\epsilon = 1$) from which we can immediately see that the change in sign occurs between $n=1$ and $n=2$. As a result we obtain that the fixed point $\gamma^* = \gamma_C$ is stable in the case $n=1$ only and that for all other order parameter component numbers $n \geqslant 2$ the stable fixed point is $\gamma^*=0$. The stability properties of the fixed points strongly change with the step from one-loop to two-loop calculation, especially for physically relevant systems with $n=2$ and $n=3$. As long as only the static critical behavior is considered, the secondary coupling γ is of less importance because the critical behavior is completely determined by the fourth-order coupling u. The stable fixed point in ϵ expansion is the Heisenberg fixed point $u^* = u_H$ for all n. With respect to the critical dynamics of model C the fixed-point value of the stable static coupling γ is most important since it governs the interaction of the two modes. These considerations are corroborated by higher-loop order calculations [26]. The borderline curve—where $\omega_c(n, \epsilon) = 0$—has been discussed in [27] using resummation procedures.

For dynamical calculations a two-loop perturbation expansion is essential. Moreover, as far as the stability of the fixed points of the time scale ratio w (or ρ) is concerned, it shows a similar strong dependence on the order of perturbation expansion, as the fixed-point structure discussed in the previous subsection.

2. Stability of the dynamic fixed points

Within dynamics there are differences in the transient exponent in model C and model C^*; however, inserting $w''^* = 0$ one obtains Eq. (63). Therefore, the dynamic transient exponent

$$\omega_w \equiv \left.\frac{\partial \beta_w}{\partial w}\right|_{\{\alpha_i\}=\{\alpha_i^*\}} \tag{72}$$

defines by the condition $\omega_w > 0$ the stability region of the dynamic fixed point w^* for a given static fixed point u^* and γ^*. In order to include the fixed point $w^* = \infty$ it is convenient to consider the parameter ρ defined in Eq. (49) instead of w, leading to a stability condition

$$\omega_\rho \equiv \left.\frac{\partial \beta_\rho}{\partial \rho}\right|_{\{\alpha_i\}=\{\alpha_i^*\}} > 0. \tag{73}$$

The two transient exponents are related by

$$\omega_\rho = \omega_w - 2\rho^* \zeta_w(u^*, \gamma^*, \rho^*) \tag{74}$$

and therefore coincide for the fixed points $\rho^* \neq 1$ (w^* finite). From Eq. (52) we obtain immediately

$$\frac{\partial \beta_\rho}{\partial \rho}(u,\gamma,\rho) = (1-2\rho)\zeta_w(u,\gamma,\rho) + \rho(1-\rho)\frac{\partial \zeta_w}{\partial \rho}(u,\gamma,\rho), \tag{75}$$

where ζ_w has been given in Eq. (50). From the same equation one gets

$$\begin{aligned}\frac{\partial \zeta_w}{\partial \rho}(u,\gamma,\rho) = \gamma^2 \Bigg\{ & 1 - \frac{n+2}{6}u(1-L) \\ & - \rho\gamma^2 \left[\frac{n}{2} - \rho - \frac{n+2}{2}L + (1+\rho)\ln(1-\rho^2) \right] \\ & + \frac{1}{2}\rho^2\gamma^2 \left(\frac{1+\rho}{1-\rho} - \ln(1-\rho^2) \right) \Bigg\}. \end{aligned} \tag{76}$$

According to the determination of the fixed points, the dynamic transient exponent can be calculated in Eq. (72) or (73), respectively, by using either the ϵ-expanded fixed-point values or the fixed-point values found by direct solution of Eq. (47). From Table I it can be seen that in the case $u^* = u_H$ we have to consider the transient exponents of five fixed points.

a. Stability of the fixed points in one-loop order. As already mentioned earlier the fixed points and also their stability regions depend strongly on the order of the loop expansion. One-loop order represents a degenerated situation in some sense because the ζ function (21) and its derivative (76) reduce to

$$\zeta_w = \left(\rho - \frac{n}{2}\right)\gamma^2, \quad \frac{\partial \zeta_w}{\partial \rho} = \gamma^2, \tag{77}$$

lacking any u contribution. In the case $\gamma^* = 0$ both functions vanish independent of ρ or w, respectively. Thus all values within the intervall [0, 1] are allowed fixed-point values for ρ, giving a line of fixed points, and $\omega_\rho = 0$ for all of them, making a statement to the stability impossible. In the case $\gamma^{*2} = \gamma_C^2$ we have the three fixed points $\rho^* = 0$ ($w^* = 0$), $\rho^* = \rho_C$ ($w^* = w_C$), and $\rho^* = 1$ ($w^* = \infty$) with $\rho_C = n/2$ [$w_C = n/(2-n)$]. Inserting these values together with Eqs. (77) into Eq. (73) the one-loop transient exponents read

TABLE II. Stability of the fixed points of model *C* in one-loop order.

u^*	γ^*	ρ^*	Region
u_H	0	$0 \leqslant \rho^* \leqslant 1$	?
	γ_C	0	Unstable
		ρ_C	$n \leqslant 2$
		1	$2 < n < 4$

$$\omega_{\rho=0} = -\frac{n}{2}\gamma_C^2, \quad \omega_{\rho=\rho_C} = \frac{n}{2}\left(1 - \frac{n}{2}\right)\gamma_C^2,$$

$$\omega_{\rho=1} = -\left(1 - \frac{n}{2}\right)\gamma_C^2, \tag{78}$$

with the static one-loop fixed-point value

$$\gamma_C^2 = \frac{2(4-n)}{n(n+8)}\epsilon. \tag{79}$$

A survey over the stability regions obtained from Eqs. (78), which are valid for arbitrary ϵ, is given in Table II.

b. Stability of the fixed points in two-loop order. The situation sketched in Table II changes drastically when the two-loop expressions of the ζ and β functions are considered. The degeneration mentioned above is now resolved and the stability regions change to a behavior which can also be expected to be valid in higher-loop orders.

Let us consider at first the case $\gamma^* = 0$ which has been completely undetermined in one-loop order regarding the fixed-point values as well as the stability. According to the previous subsection in two-loop order only the two fixed-point values $\rho^* = 0$ and $\rho^* = 1$ remain from the line of fixed points. At vanishing γ only the model *A* contributions remain in the dynamic ζ function which is independent of the value of ρ^*. The ζ function (21) reduces to $\zeta_\Gamma^{(A)}(u)$, valid in all orders of perturbation expansion. Thus we obtain from Eq. (75) immediately

$$\omega_{\rho=0}^{(0)} = \zeta_w(u_H,0,0) = c\,\eta, \quad \omega_{\rho=1}^{(0)} = -\zeta_w(u_H,0,1) = -c\,\eta. \tag{80}$$

In two-loop order we have [28,29]

$$c\,\eta = \frac{n+2}{36}u_H^2\left(L - \frac{1}{2}\right), \tag{81}$$

where the ϵ-expanded expression is obtained when the Heisenberg fixed-point value u_H from Eq. (42) is inserted in first order. The above quantity is always positive since it is an anomalous dimension in an unitary field theory [30]. Therefore the fixed point $\rho^* = 1$ is always unstable. The stability region of $\rho^* = 0$ is determined by $\omega_c = 0$; with Eq. (71), we obtain the *stability* boundary

$$\epsilon_\alpha(n)=\frac{(4-n)(n+8)^2}{(n+2)(13n+44)} \tag{82}$$

in the ϵ-n plane. From Eqs. (69) and (70) it is evident that the curve (82) separates the region with stable finite fixed-point value $\gamma^*=\gamma_C$ from the region with stable fixed-point value $\gamma^*=0$, or in other words the stability boundary is the line where the specific heat exponents changes sign.

In the second case, when $\gamma^*=\gamma_C$, three dynamic fixed points exist as shown in Table I. At vanishing ρ the ζ function (21) reduces to $\zeta_w(u,\gamma_C,0)=1/2[\zeta_\psi(u)-\zeta_{\bar{\psi}^\dagger}(u,\gamma,0)]-\zeta_\lambda(u,\gamma)=\zeta_\Gamma^{(A)}(u)-\zeta_\lambda(u,\gamma)$ which is also valid in all orders of perturbation expansion. With Eq. (19) this leads to the transient exponent

$$\omega_{\rho=0}^{(C)}=\zeta_w(u_H,\gamma_C,0)=c\,\eta-\gamma_C^2 B_{\psi^2}(u_H). \tag{83}$$

With the two-loop results (81) for $c\,\eta$ and $B_{\psi^2}(u_H)=n/2$ the condition $\omega_{\rho=0}^{(C)}=0$ leads to the stability boundary curve

$$\epsilon_{st}(n)=\frac{(4-n)(n+8)}{(n+2)\left[\dfrac{13n+44}{n+8}+\left(L-\dfrac{1}{2}\right)\right]}\equiv\epsilon_1(n), \tag{84}$$

with the two-loop fixed-point values u_H and γ_C inserted. One sees that the *stability* border line between the fixed point $\rho^*\neq 0$ and $\rho^*=0$ coincides with the *existence* borderline of the nonzero fixed point to all orders of perturbation theory since Eq. (83) is identical to Eq. (57). Moreover, the stability boundary condition is equivalent to the equality of the dynamical critical exponents z of the adjoining regions (here region II and region I_b). This condition was used in [15].

Equation (84) defines together with the boundary (82) three different regions in the ϵ-n plane in which different fixed points (u^*,γ^*,ρ^*) are stable (see Fig. 1):

(i) region I_a: right to $\epsilon_\alpha(n)$ with $(u_H,0,0)$ stable,
(ii) region I_b: between $\epsilon_1(n)$ and $\epsilon_\alpha(n)$ with $(u_H,\gamma_C,0)$ stable,
(iii) region II: left to $\epsilon_1(n)$ with (u_H,γ_C,ρ_C) stable.

In region I_a the conserved density *decouples* from the nonconserved OP. In region I_b the densities are coupled but the OP scales with $z=2+c\,\eta$ [31] and the conserved density with $z_m=2+\alpha/\nu$. Thus one may call this region the weak-scaling region. In region II both densities scale with the *same* dynamical critical exponent $z=2+\alpha/\nu$ different from model *A*.

At $\rho^*=1$ $(w^*=\infty)$ one obtains from Eq. (50)

$$\omega_{\rho=1}^{(C)}=-\zeta_w(u_H,\gamma_C,1)\sim\lim_{\rho\to 1}\ln(1-\rho^2)\to-\infty, \tag{85}$$

from which it is evident that this fixed point is always unstable.

In order to obtain the transient exponent for the finite fixed-point value $\rho^*=\rho_C$ we have to calculate

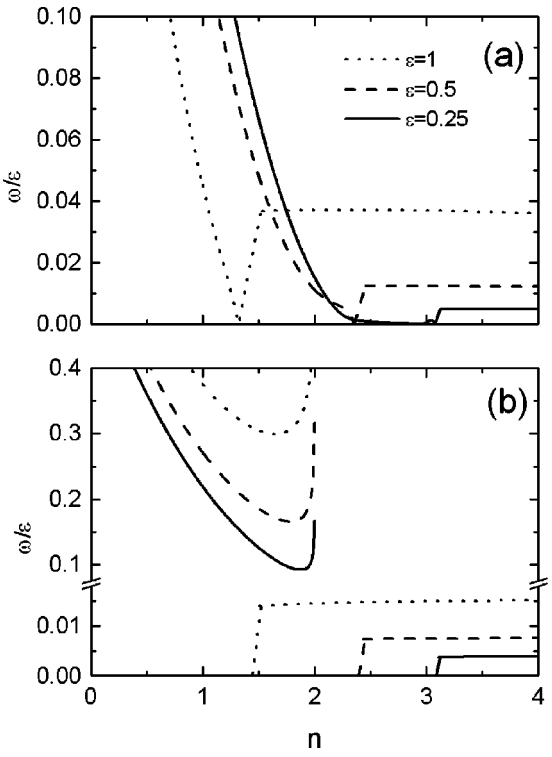

FIG. 3. Dynamic stability function $\omega(\epsilon,n)$ divided by ϵ for various ϵ (a) for the nonlinear fixed point Eq. (73) and (b) for the ϵ-expanded solution. The curves consist of the different parts corresponding to the stable fixed points (see text).

$$\omega_{\rho=\rho_C}^{(C)}=(1-2\rho_C)\zeta_w(u_H,\gamma_C,\rho_C)+\rho_C(1-\rho_C)\frac{\partial\zeta_w}{\partial\rho}(u_H,\gamma_C,\rho_C) \tag{86}$$

explicitly. This can be done either by using a strict ϵ expansion or by a nonlinear calculation using the fixed-point values of ρ found by direct solution of the equation $\beta_\rho=0$.

Inserting Eq. (54) into Eq. (73) systematically in the ϵ expansion we obtain the ϵ-expanded result for the transient exponent:

$$\omega_{\rho=\rho_C}^{(C)}=\frac{\epsilon}{2(n+8)}\left((2-n)(4-n)+\frac{n+2}{n+8}\epsilon\left[(2L-1)-\frac{(2-n)(13n+44)}{n+8}\right]+(4-n)\epsilon\left\{2(2-n)b_c-\frac{(4-n)(n+2)}{n+8}\left[(4-n)\left(\frac{1}{4}-L\right)+\left[3-n+\frac{n(2-n)}{4(n+2)}\right]\ln\left(1-\frac{n^2}{4}\right)\right]\right\}\right). \tag{87}$$

It turns out that Eq. (87) is positive in the whole existence region of the ϵ-expanded fixed point $\rho^*=\rho_C$ [see Fig. 3(b)]. This is also the case for the corresponding existence region, when ω_{ρ_C} is calculated from the nonlinear equation without ϵ expansion, which is shown in Fig. 3(a) at several ϵ. The

transient exponent discussed so far is valid in the region where the fixed point (u_H, γ_C, ρ_C) is stable. However, in the ϵ expansion it turns out that within the stability region of $\rho^* = \rho_C$ there may be other stable fixed points present depending on the dimension. From Fig. 1 one can see that at constant ϵ the stable fixed point first changes to $(u_H, \gamma_C, 0)$ at $\epsilon_1(n)$ and then to $(u_H, 0, 0)$ at $\epsilon_\alpha(n)$. The corresponding transient exponents of these two additional fixed points are also drawn in Fig. 3(b) in the corresponding region of stability. Such a situation does not appear when one solves the nonlinear equations [see Fig. 3(a)]. The existence regions and the stability regions of the different fixed points then join neatly.

In Fig. 3(a) one can see that the transient exponent drops down to zero at the existence boundary, indicating the stability boundary. For small values of ϵ in the region where the fixed-point value is nearly 1 [see Fig. 2(a)] the transient exponent also drops down to very small values. In this region we cannot calculate the transient exponent numerically but analytically. From the asymptotic solution ρ_{as} in Eq. (58) we can calculate the asymptotic transient exponent $\omega_\rho^{(as)}$ as

$$\omega_\rho^{(as)}(\epsilon, n) = \gamma^{*4} + x\gamma^{*2}\left[1 - \frac{n+2}{6}u^*(1-L) - \gamma^{*2}\left(\frac{n}{2} - 1 - \frac{n+2}{2}L + \frac{5}{2}\ln 2x\right)\right], \quad (88)$$

showing that the transient exponent always remains positive. The detailed behavior within this region has been shown in Fig. 3(b) of Ref. [18].

A numerical calculation of the dynamic transient exponents at some points in the ϵ-n space where real experiments can be expected, which are $\epsilon = 1$ at $n = 1$, $n = 2$, and $n = 3$, reveals that in the case of $n = 2$ and $n = 3$ its value is very small—namely, 0.0145 ($n = 2$) and 0.015 ($n = 3$). For $n = 1$ we obtain 0.045. Thus the fixed-point value $w^* = 0$ will be only reached very slowly, but this is true even for $w^* = w_C$ as shown in the next section.

V. FLOW OF THE MODEL *C* PARAMETERS

The behavior of the flow at different order parameter component numbers n is demonstrated in Fig. 4. The flows of the static parameter γ^2 and the time scale ratio w are plotted at $\epsilon = 1$ at several n. In all cases the same initial values $\gamma^2(l_0)$ and $w(l_0)$ have been chosen. For $n = 1$ the flow tends to the stable finite fixed-point values $\gamma^{*2} = \gamma_C^2$ and $w^* = w_C$. The other two cases ($n = 2$ and $n = 3$) have to reach the fixed-point values $\gamma^* = 0$ and $w^* = 0$. While $\gamma^2(l)$ decreases relatively fast to its fixed-point value, the time scale ratio $w(l)$ has not reached it even at a flow parameter value $l = 10^{-40}$. Thus the nonasymptotic behavior of w extends over the whole region plotted in Fig. 4 and cannot be neglected therein. Recalling that experiments can been performed to temperature distances which correspond to flow parameter values of $l = 10^{-10}$ at best, it is obvious that their results are far away of any asymptotic behavior.

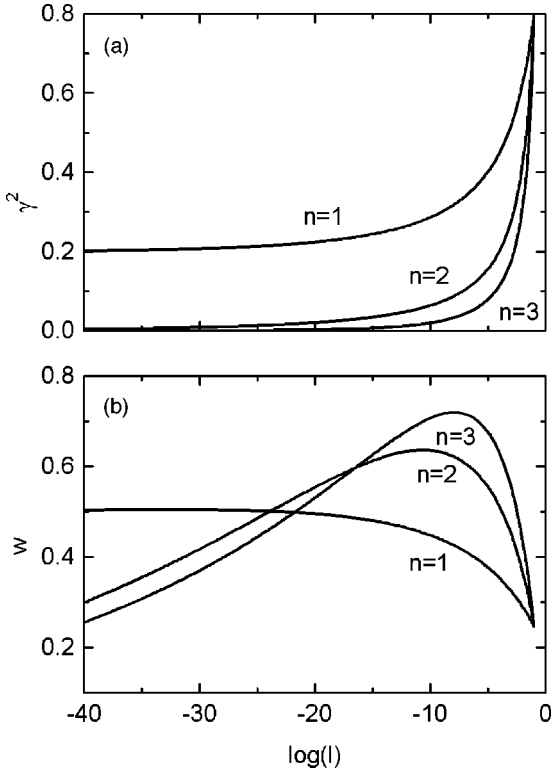

FIG. 4. Flow of (a) the static parameter γ^2 and (b) the time scale ratio w at $\epsilon = 1$ ($d = 3$) at three physically relevant order parameter component numbers $n = 1, 2, 3$. The initial values $\gamma^2(l_0) = 0.8$ and $w(l_0) = 0.246$ are the same in all three cases. [$\log(l) = \log_{10}(l)$].

The case $n = 1$ is considered in more detail in Fig. 5. The flow for γ^2 is plotted [Fig. 5(a)] for three different initial conditions, one where the parameter starts at its fixed-point value (the result has clearly to be a constant) and two with deviating values. To each of the γ^2 flows three flows of the dynamic scale ratio with different initial conditions $w(l_0)$ are drawn in Fig. 5(b). Analogous to the static parameter γ one initial value of w is the fixed-point value. The remaining two initial values are $w(l_0) = w^*/10$ and $w(l_0) = 2w^*$. When γ^2 and w start at their fixed-point values the resulting w flow is a constant, which is a test for the correctness of the flow equations. At deviating initial conditions $\gamma^2(l_0) \neq \gamma^*$ the flow of w drifts away from its fixed-point value at first even when it starts precisely on it. This is because the nonasymptotic behavior of γ^2 couples into the flow equation of w.

In Fig. 6 the influence of the imaginary part of w in the complex model C^* on the flow of the real part of w is examined. There we have compared the flow of w calculated from the flow equation (27) using the ζ function from the real model C with the flow of w' calculated within the complex model C^*. The initial values $w(l_0)$ and $w'(l_0)$ are the same; thus, the corresponding curves start from the same point in Fig. 6. In the complex model C^* the imaginary part couples into the flow equation for the real part of w, resulting in a considerable deviation in $w'(l)$ compared to $w(l)$ in the

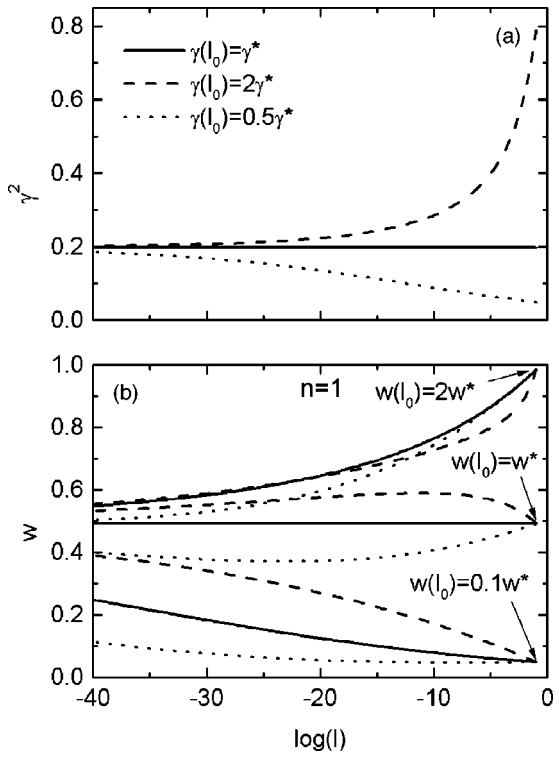

FIG. 5. Flow of (a) the static parameter γ^2 and (b) the time scale ratio w at $\epsilon=1$ ($d=3$), $n=1$ for different initial values $\gamma^2(l_0)$ and $w(l_0)$. [$\log(l)=\log_{10}(l)$].

real case. Due to the appearance of a zero eigenvalue [see Eq. (63)], the decay is logarithmically slow and leads to large differences between the flows of w and w'.

The general result for all cases $n=1,2,3$ is that applying model C to a physical system one has to expect nonasymptotic behavior. This is also seen from the small transient exponents (which are equal to the stability exponents) in two-loop order.

VI. COMPARISON WITH THE RESULTS OF OTHER AUTHORS

The ζ functions ζ_Γ, and ζ_w, respectively, have been calculated so far by several authors within the field-theoretic renormalization group theory. Actually two results exist which have been published in the literature. The first result was published by Brezin and De Dominicis [13] in 1975 for arbitrary n and the second one was published by Dohm [19] within his calculation of model F (critical dynamics of ^{4}He) in 1991 for the special case $n=2$. The results obtained by these authors are different from each other and also different from our result.

A. Results of Brezin and De Dominicis

Rewriting the result of Brezin and De Dominicis [13] by the use of our definitions to our notation, the dynamic ζ function obtained by these authors reads [32]

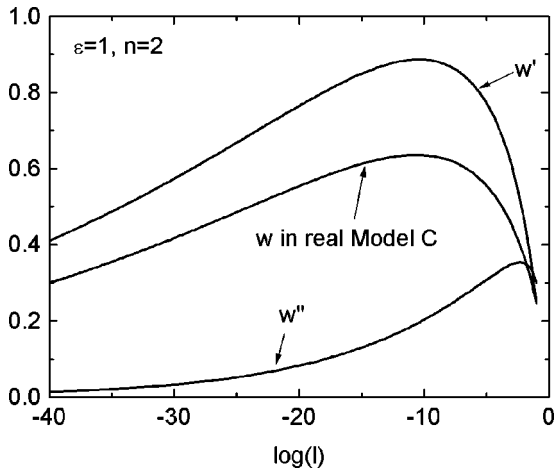

FIG. 6. w flow of the real model C compared to the flow of w' and w'' of the complex model C^* at $\epsilon=1$, $n=2$. The initial values are chosen as $w(l_0)=w'(l_0)=0.246$ and $w''(l_0)=0.3$. [$\log(l)=\log_{10}(l)$].

$$\zeta_w^{(BD)}(u,\gamma,\rho)=\left(\rho-\frac{n}{2}\right)\gamma^2-\frac{1}{2}\rho\gamma^2\Bigg[-\frac{n+2}{3}u(1+L+\ln\rho)+\rho\gamma^2\left(\frac{n}{2}\frac{1-2\rho}{\rho}-\rho-\frac{n+2}{2}L(1+\rho)\times\ln(1-\rho^2)-\frac{n}{2}\ln\rho\right)\Bigg]+\frac{n+2}{36}u^2\left(L-\frac{1}{2}\right). \tag{89}$$

A comparison with Eq. (50) reveals several differences between the two expressions ranging from different signs over different ρ terms to additional $\ln\rho$ terms, which lead to a completely different behavior in the fixed-point function $\rho^*=\rho_C(\epsilon,n)$ and also in the derivative of ζ_w and therefore in the transient exponents. At small ϵ and large n Eq. (89) has fixed-point solutions which are qualitatively similar to our solutions. But at larger ϵ or small n their fixed-point solu-

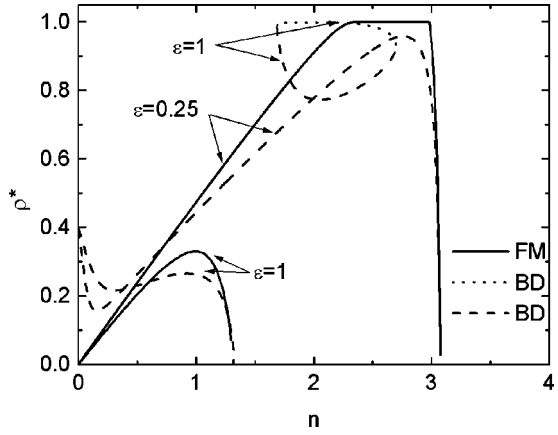

FIG. 7. Comparison of the solution for the fixed-point values following from our ζ function (solid lines) and from the ζ function obtained by Brezin and De Dominicis (dashed and dotted lines) at two different values for ϵ.

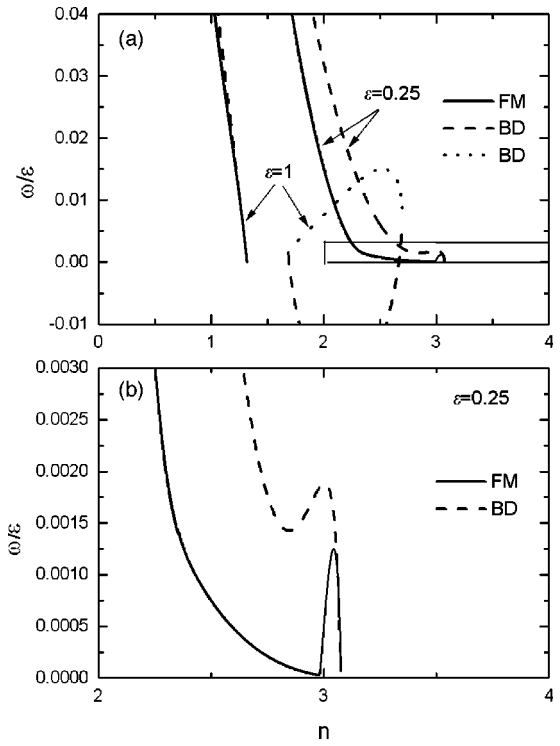

FIG. 8. (a) Comparison of the solution for the transient exponent following from our ζ function (solid lines) and from the ζ function obtained by Brezin and De Dominicis (BD) (dashed and dotted lines) at two different values for ϵ. The two fixed-point solutions of BD at $\epsilon=1$ lead to two transient exponents (compare Fig. 7). (b) The region marked in (a) enlarged for $\epsilon=0.25$.

tions differ considerably from ours, leading to discontinuous functions which also have a region where two finite fixed-point values exist simultaneously. This is demonstrated in Fig. 7 where we have compared our fixed-point solution at $\epsilon=1$ and $\epsilon=0.25$ with the solutions obtained from Eq. (89). At larger ϵ values the ζ function (89) of Brezin and De Dominicis produces fixed-point solutions in regions where we do not have any solutions. In Fig. 7 one can see that at $\epsilon=1$ two fixed points exist simultaneously (dashed and dotted lines) in the region $1.5<n<3$, while our solution (solid line) does not exceed $n=1.5$. Near $n=0$ the fixed-point values show a strong increase instead of going to zero. Thus the two-loop results of [13] do not converge in the limit $\epsilon\to 0$ to the one-loop result in a simple manner. The resulting differences in the transient exponent are plotted in Fig. 8.

The different ζ functions lead to a flow, calculated from Eq. (27) with Eq. (89), which deviates considerably from the flow calculated with our ζ function. As an example we have plotted in Fig. 9 both flows for $\epsilon=1$, $n=1$ starting at the same initial values.

B. Results of Dohm

The difference between our result and the result of Dohm is considerably weaker in the explicit expression of the ζ function (no additional $\ln\rho$ contributions) on one side, but also in the behavior of the flow or the fixed-point values. The latter is due to the fact that his ζ function has been calculated

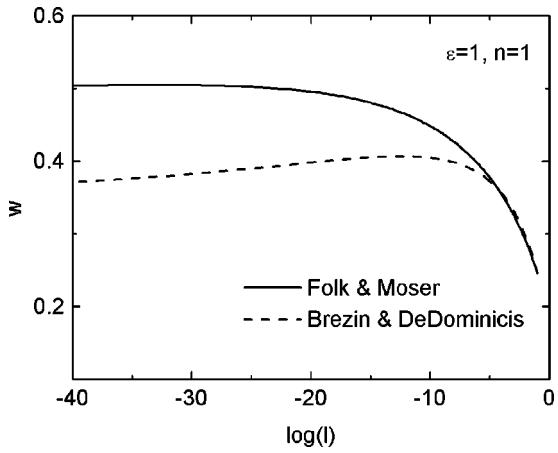

FIG. 9. Comparison of the flow of w following from our ζ function (solid line) and from the ζ function obtained by Brezin and De Dominicis (dashed line) at $\epsilon=1$, $n=1$. $[\log(l)=\log_{10}(l)]$.

only at $n=2$ where the stable fixed point is $w^*=0$ anyway. Rewriting Dohm's ζ function $\zeta_w^{(\mathrm{Dohm})}(u,\gamma,\rho)$ [19] to our notation we get

$$\zeta_w^{(\mathrm{Dohm})}(u,\gamma,\rho)=\zeta_w(u,\gamma,\rho)+\frac{1}{12}(3\rho-2)(1-\rho)\gamma^4 L. \tag{90}$$

$\zeta_w(u,\gamma,\rho)$ is in this case (50) taken at $n=2$. Qualitatively the main difference between our's and Dohm's result is that our result (50) turns into the ζ function of model A in the limit $\rho\to 0$ (corresponding to the limit $w\to 0$) even when γ is not zero, while Dohm's result does not have this property because of the additional term in Eq. (90). Thus for $n=2$ in the asymptotic limit the models coincide but not in the non-asymptotic region. This is seen in the differences in the flow of the time scale ratio w at $\epsilon=1$ in Fig. 10. For comparison we have also plotted the flow obtained with the ζ function of Brezin and De Dominicis.

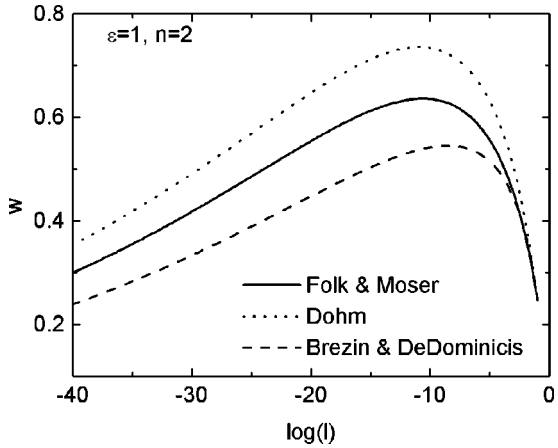

FIG. 10. Comparison of the solution of the flow equation (27) using our (solid line), Dohm's (dotted line), and Brezin and De Dominicis' (dashed line) ζ function at $\epsilon=1$, $n=2$ with the same initial values. $[\log(l)=\log_{10}(l)]$.

VII. CONCLUSION

For applications of model C as discussed in the Introduction, it is important to get consistent results for the fixed points and their stability regions, because the fixed points characterize the critical behavior. We have shown that model C has no anomalous properties apart from the fact that due to an essential singularity in ϵ the ϵ expansion of the fixed point of the time scale ratio w_C breaks down. This can be repaired by solving the fixed-point equation without expansion. Then the results for the stability regions and the fixed points itself show a consistent and continuous picture in the sense that at the borderlines the exponents and fixed points are continuous.

Model C^*/C is also a limiting case of more complicated models, like model F, describing the critical dynamics at the superfluid transition of ^{4}He and the planar antiferromagnet, and model F', describing the critical dynamics at the superfluid transition in ^{3}He-^{4}He mixtures. Therefore, the explicit results for the renormalization group functions are important test functions for the more complicated models. The model C functions agree with this limit when the recent results [16] for the more complicated models are used.

The flow of the dynamical parameters to their fixed-point values turns out to be slow because of the small values of the transient exponents found in two-loop order. This has to be taken into account when using these parameters for calculating physical quantities even in systems with OP components $n=2$, 3 (in $d=3$) for which the conserved density decouples asymptotically.

The small values of the dynamical transient exponents may be important even for $n=1$ and should be considered in the interpretation of computer simulations [38]. It might happen that one has not reached asymptotics and finds effective exponents in the analysis of the data. More work in this direction would be desirable.

ACKNOWLEDGMENT

This work was supported by the Fonds zur Förderung der wissenschaftlichen Forschung under Project No. 15247-TPH.

APPENDIX A: PERTURBATION EXPANSION

1. Dynamic functional

Following [33] the dynamic equations (1) and (3) together with Eq. (6) lead to a dynamic functional of the form $J=J_0+J_{int}$ with the Gaussian part J_0 given by

$$J_0=\int dt\int dx\Big\{-4\mathring{\Gamma}'\vec{\tilde{\psi}}_0\cdot\vec{\tilde{\psi}}_0^\dagger+\mathring{\lambda}_m\tilde{m}_0\nabla^2\tilde{m}_0 + \vec{\tilde{\psi}}_0^\dagger\cdot\left(\frac{\partial}{\partial t}+\mathring{\Gamma}(\mathring{\tau}-\nabla^2)\right)\vec{\psi}_0+\vec{\tilde{\psi}}_0\left(\frac{\partial}{\partial t}+\mathring{\Gamma}^\dagger(\mathring{\tau}-\nabla^2)\right)\vec{\psi}_0^\dagger + \tilde{m}_0\left(\frac{\partial}{\partial t}-a_m\mathring{\lambda}_m\nabla^2\right)m_0\Big\} \tag{A1}$$

and an interaction part which is

$$J_{int}=\int dt\int dx\Big\{\mathring{\Gamma}\frac{\mathring{\tilde{u}}}{3!}(\vec{\tilde{\psi}}_0^\dagger\cdot\vec{\psi}_0)(\vec{\psi}_0^\dagger\cdot\vec{\psi}_0)+\mathring{\Gamma}^\dagger\frac{\mathring{\tilde{u}}}{3!}(\vec{\tilde{\psi}}_0\cdot\vec{\psi}_0^\dagger) \times(\vec{\psi}_0\cdot\vec{\psi}_0^\dagger)+\mathring{\Gamma}\,\mathring{\gamma}_m m_0(\vec{\tilde{\psi}}_0^\dagger\cdot\vec{\psi}_0)+\mathring{\Gamma}^\dagger\mathring{\gamma}_m m_0(\vec{\tilde{\psi}}_0\cdot\vec{\psi}_0^\dagger) -\frac{1}{2}\mathring{\lambda}_m\mathring{\gamma}_m\tilde{m}_0\nabla^2(\vec{\psi}_0\cdot\vec{\psi}_0^\dagger)\Big\}. \tag{A2}$$

The centerdot denotes an $(n/2)$-dimensional scalar product. $\vec{\tilde{\psi}}_0$ and $\tilde{m}_0$ represent auxiliary densities.

2. Dynamic order parameter vertex functions

Within the dynamic approach of Bausch, Janssen, and Wagner [33], two dynamic vertex functions exist, which correspond to the order parameter.

The first one $\mathring{\Gamma}_{\psi\tilde{\psi}^\dagger}(\xi,k,\omega)$ is related to the response function. Calculating the perturbation expansion up to two-loop order the vertex function mentioned is obtained from the dynamic functionals (A1) and (A2). It turns out that it has the structure

$$\mathring{\Gamma}_{\psi\tilde{\psi}^\dagger}(\xi,k,\omega)=-i\omega\mathring{\Omega}_{\psi\tilde{\psi}^\dagger}(\xi,k,\omega)+\mathring{\Gamma}_{\psi\psi^\dagger}(\xi,k)2\mathring{\Gamma}, \tag{A3}$$

where $\mathring{\Gamma}_{\psi\psi^\dagger}(\xi,k)$ is the static two-point vertex function. In the above expression the correlation length $\xi(\mathring{r},\mathring{u})$, which is defined as

$$\xi^{-2}(\mathring{r},\mathring{u})=\left.\frac{\partial\ln\mathring{\Gamma}_{\psi\psi^\dagger}(\mathring{r},\mathring{u},k)}{\partial k^2}\right|_{k=0}, \tag{A4}$$

already has been introduced by collecting the proper perturbational contributions of ξ. The static vertex function $\mathring{\Gamma}_{\psi\psi^\dagger}(\mathring{r},\mathring{u},k)$ is calculated from the Ginzburg-Landau-Wilson model (7) with complex order parameter. The dynamic function $\mathring{\Omega}_{\psi\tilde{\psi}^\dagger}$ reads in two-loop order

$$\mathring{\Omega}_{\psi\tilde{\psi}^\dagger}(\xi,k,\omega)=1+\mathring{\Gamma}\,\mathring{\gamma}^2 I_C(\xi,k,\omega)+\mathring{\Omega}^{(2L)}_{\psi\tilde{\psi}^\dagger}(\xi,k,\omega), \tag{A5}$$

with the rescaled coupling $\mathring{\gamma}=\mathring{\gamma}_m/\sqrt{a_m}$. The two-loop contributions have the structure

$$\mathring{\Omega}^{(2L)}_{\psi\tilde{\psi}^\dagger}(\xi,k,\omega)=\frac{n+2}{18}\mathring{\Gamma}\mathring{u}^2\mathring{W}^{(A)}_{\psi\tilde{\psi}^\dagger}(\xi,k,\omega) -\frac{n+2}{3}\mathring{\Gamma}\mathring{u}\,\mathring{\gamma}^2\mathring{C}^{(T3)}_{\psi\tilde{\psi}^\dagger}(\xi,k,\omega) +\mathring{\Gamma}\,\mathring{\gamma}^4\mathring{S}_{\psi\tilde{\psi}^\dagger}(\xi,k,\omega), \tag{A6}$$

with

$$\mathring{S}_{\psi\tilde{\psi}^\dagger}(\xi,k,\omega)=\mathring{C}^{(T4)}_{\psi\tilde{\psi}^\dagger}(\xi,k,\omega)+\frac{n}{2}[\mathring{C}^{(T5)}_{\psi\tilde{\psi}^\dagger}(\xi,k,\omega)-\mathring{C}^{(T3)}_{\psi\tilde{\psi}^\dagger}(\xi,k,\omega)]+\mathring{C}^{(T6)}_{\psi\tilde{\psi}^\dagger}(\xi,k,\omega)-\mathring{C}^{(T3)}_{\psi\tilde{\psi}^\dagger}(\xi,k,\omega). \tag{A7}$$

The one-loop integral I_C in Eq. (A5) reads

$$I_C(\xi,k,\omega)=\int_{k'}\frac{1}{[\xi^{-2}+(k+k')^2](-i\omega+\alpha')}, \tag{A8}$$

with α' defined by

$$\alpha'=\mathring{\Gamma}[\xi^{-2}+(k+k')^2]+\mathring{\lambda}k'^2. \tag{A9}$$

The first two-loop contribution in Eq. (A6) comes from the well-known model *A*. $\mathring{W}^{(A)}_{\psi\tilde{\psi}^\dagger}$ is given by

$$\mathring{W}^{(A)}_{\psi\tilde{\psi}^\dagger}(\xi,k,\omega)=\int_{k'}\int_{k''}\frac{1}{(\xi^{-2}+k'^2)(\xi^{-2}+k''^2)[\xi^{-2}+(k+k'+k'')^2](-i\omega+A)}, \tag{A10}$$

with

$$A=\mathring{\Gamma}(\xi^{-2}+k'^2)+\mathring{\Gamma}^\dagger(\xi^{-2}+k''^2)+\mathring{\Gamma}[\xi^{-2}+(k+k'+k'')^2]. \tag{A11}$$

The remaining two-loop contributions in Eqs. (A6) and (A7) are marked with superscripts (*Ti*), which indicate the final expressions of different graphical topologies after all the rearrangements have been done. They are

$$\mathring{C}^{(T3)}_{\psi\tilde{\psi}^\dagger}(\xi,k,\omega)=\int_{k'}\int_{k''}\frac{1}{[\xi^{-2}+(k+k')^2](-i\omega+\alpha')(-i\omega+A)}\times\left(\frac{\mathring{\Gamma}}{\xi^{-2}+k''^2}+\frac{\mathring{\Gamma}^\dagger}{\xi^{-2}+(k'+k'')^2}\right), \tag{A12}$$

$$\mathring{C}^{(T4)}_{\psi\tilde{\psi}^\dagger}(\xi,k,\omega)=\int_{k'}\int_{k''}\frac{\mathring{\Gamma}^2}{[\xi^{-2}+(k+k'+k'')^2](-i\omega+\alpha')^2(-i\omega+\beta)}, \tag{A13}$$

$$\mathring{C}^{(T5)}_{\psi\tilde{\psi}^\dagger}(\xi,k,\omega)=\int_{k'}\int_{k''}\frac{\mathring{\lambda}k'^2}{[\xi^{-2}+(k+k')^2](-i\omega+\alpha')^2(-i\omega+A)}\times\left(\frac{\mathring{\Gamma}}{\xi^{-2}+k''^2}+\frac{\mathring{\Gamma}^\dagger}{\xi^{-2}+(k'+k'')^2}\right), \tag{A14}$$

$$\mathring{C}^{(T6)}_{\psi\tilde{\psi}^\dagger}(\xi,k,\omega)=\int_{k'}\int_{k''}\frac{\mathring{\lambda}k''^2}{[\xi^{-2}+(k+k')^2](-i\omega+\alpha')(-i\omega+\alpha'')(-i\omega+A')}\left(\frac{\mathring{\Gamma}}{\xi^{-2}+(k+k'+k'')^2}+\frac{\mathring{\Gamma}^\dagger}{\xi^{-2}+(k+k'')^2}\right)+\int_{k'}\int_{k''}\frac{\mathring{\Gamma}}{[\xi^{-2}+(k+k')^2](-i\omega+\alpha'')(-i\omega+\beta)}\left[\frac{\mathring{\Gamma}}{-i\omega+\alpha'}+\frac{1}{\xi^{-2}+(k+k'+k'')^2}\left(1+\frac{\mathring{\lambda}k''^2}{-i\omega+\alpha'}\right)\right], \tag{A15}$$

where we have introduced

$$\beta=\mathring{\Gamma}[\xi^{-2}+(k+k'+k'')^2]+\mathring{\lambda}(k'^2+k''^2), \tag{A16}$$

$$A'=\mathring{\Gamma}[\xi^{-2}+(k+k')^2]+\mathring{\Gamma}^\dagger[\xi^{-2}+(k+k'+k'')^2]+\mathring{\Gamma}[\xi^{-2}+(k+k'')^2], \tag{A17}$$

which are both invariant under an interchange of k' and k''. Note that Eqs. (A7)–(A17) are obtained after a considerable rearrangement of the graphical contributions in order to get the structure of the OP vertex function, Eq. (A3), explicitly and identify the function $\Omega_{\psi\tilde{\psi}^\dagger}$.

The second dynamic vertex function $\mathring{\Gamma}_{\tilde{\psi}\tilde{\psi}^\dagger}(\xi,k,\omega)$ is necessary for the calculation of the dynamic correlation function

$$\mathring{C}_{\psi\psi^\dagger}(\xi,k,\omega)=-\frac{\mathring{\Gamma}_{\tilde{\psi}\tilde{\psi}^\dagger}(\xi,k,\omega)}{|\mathring{\Gamma}_{\psi\tilde{\psi}^\dagger}(\xi,k,\omega)|^2}. \tag{A18}$$

The correlation function is a real function; thus, from the

above relation it follows that $\mathring{\Gamma}_{\tilde{\psi}\tilde{\psi}^\dagger}(\xi,k,\omega)$ also has to be real. A calculation up to two-loop order reveals that this function fulfills the relation

$$\mathring{\Gamma}_{\tilde{\psi}\tilde{\psi}^\dagger}(\xi,k,\omega) = -4\,\mathrm{Re}[\mathring{\Gamma}\mathring{\Omega}_{\psi\tilde{\psi}^\dagger}(\xi,k,\omega)]. \tag{A19}$$

From this relation it turns out that the second dynamic vertex function is completely determined by the first one. In a calculation of the correlation function (A18) one only has to know the function $\mathring{\Omega}_{\psi\tilde{\psi}^\dagger}(\xi,k,\omega)$ and the static vertex function $\mathring{\Gamma}_{\psi\psi^\dagger}(\xi,k)$.

At least we want to remark that in the case of the real model *C*, where the complex order parameter turns into a real *n*-component vector $\vec{\phi}_0$, Eq. (A3) reads

$$\mathring{\Gamma}_{\phi\tilde{\phi}}(\xi,k,\omega) = -i\omega\mathring{\Omega}_{\phi\tilde{\phi}}(\xi,k,\omega) + \mathring{\Gamma}_{\phi\phi}(\xi,k)\mathring{\Gamma}, \tag{A20}$$

where the kinetic coefficient $\mathring{\Gamma}$ is now a real quantity. In Eq. (A20) the relation

$$\mathring{\Gamma}_{\psi\psi^\dagger}(\xi,k) = \frac{1}{2}\mathring{\Gamma}_{\phi\phi}(\xi,k) \tag{A21}$$

between the static vertex functions has been used. Correspondingly relation (A19) turns into

$$\mathring{\Gamma}_{\tilde{\phi}\tilde{\phi}}(\xi,k,\omega) = -2\mathring{\Gamma}\,\mathrm{Re}[\mathring{\Omega}_{\phi\tilde{\phi}}(\xi,k,\omega)]. \tag{A22}$$

3. ϵ poles of the integrals

In order to obtain the pole terms $\cdots_s$ we consider the integrals at vanishing frequency ω and wave vector k in a generalized form. The one-loop integral (A8) has the structure

$$I_C = \int_{k'} \frac{1}{(a+k'^2)(b+k'^2)}. \tag{A23}$$

The two-loop contributions (A10)–(A15) contain five independent two-loop integrals of the following structure:

$$I_{C_1} = \int_{k'}\int_{k''} \frac{1}{(a+k'^2)(A+k''^2)[B+(k'+k'')^2][e+\mu k'^2+\nu k''^2+(k'+k'')^2]}, \tag{A24}$$

$$I_{C_2} = \int_{k'}\int_{k''} \frac{1}{(a+k'^2)(b+k'^2)(A+k''^2)[e+\mu k'^2+\nu k''^2+(k'+k'')^2]}, \tag{A25}$$

$$I_{C_3} = \int_{k'}\int_{k''} \frac{k'^2}{(a+k'^2)(b+k'^2)^2(A+k''^2)[e+\mu k'^2+\nu k''^2+(k'+k'')^2]}, \tag{A26}$$

$$I_{C_4} = \int_{k'}\int_{k''} \frac{k''^2}{(a+k'^2)(b+k'^2)(A+k''^2)(B+k''^2)[e+\mu k'^2+\nu k''^2+(k'+k'')^2]}, \tag{A27}$$

$$I_{C_5} = \int_{k'}\int_{k''} \frac{k''^2}{(a+k'^2)(b+k'^2)(A+k''^2)[B+(k'+k'')^2][e+\mu k'^2+\nu k''^2+(k'+k'')^2]}. \tag{A28}$$

In order to obtain the dimensional pole terms, all integrals have to be calculated in the ϵ expansion. For the calculation of the *Z* factors only it is necessary to expand the one-loop integrals up to order ϵ^0 and the two-loop integrals up to order $1/\epsilon$. The one-loop integral (A23) reads

$$I_C = \frac{A_d}{\epsilon}\left\{1 - \frac{\epsilon}{2}\frac{a\ln a - b\ln b}{a-b}\right\} + O(\epsilon). \tag{A29}$$

For convenience we have introduced the geometry factor

$$A_d = \Gamma\left(1-\frac{\epsilon}{2}\right)\Gamma\left(1+\frac{\epsilon}{2}\right)\frac{\Omega_d}{(2\pi)^d}, \tag{A30}$$

with *d* the space dimension, Ω_d the surface of the *d*-dimensional unit sphere, and $\Gamma(x)$ the Euler Γ function.

For the first two-loop integral I_{C_1} we obtain

$$[I_{C_1}]_S = \frac{A_d^2}{4\epsilon}\left\{\frac{1}{\mu}\ln\frac{(1+\mu)(\mu+\nu)}{\mu+\nu+\mu\nu} + \frac{1}{\nu}\ln\frac{(1+\nu)(\mu+\nu)}{\mu+\nu+\mu\nu} + \ln\frac{(1+\mu)(1+\nu)}{\mu+\nu+\mu\nu}\right\}. \tag{A31}$$

Note that in the case $\mu=\nu=1$ and $a=A=B=e=\xi^{-2}/\kappa^2$ the above integral reduces to the integral appearing in the well-known model *A* (pure relaxation model without mode coupling terms and without secondary densities). Inserting this into the above result we obtain $I_{C_1}(\mu=\nu=1) = (3A_d^2/4\epsilon)\ln 4/3$, which is consistent with previous calculations.

The pole terms of the second integral I_{C_2}, Eq. (A25), and the fourth integral, Eq. (A27), are equal. They read

$$[I_{C_2}]_S=[I_{C_4}]_S=\frac{A_d^2}{2\epsilon^2(1+\nu)}\left\{1+\frac{\epsilon}{2}\left[1+\ln\frac{1+\nu}{1+\mu}-\sigma\ln\frac{1+\sigma}{\sigma}\right]-\epsilon\frac{a\ln a-b\ln b}{a-b}\right\}, \tag{A32}$$

where we have introduced $\sigma=\mu+\nu+\mu\nu$. The above results for Eqs. (A31) and (A32) are also consistent with the results given by Dohm in his model F calculation. The pole terms of Eqs. (A26) and (A28) read

$$[I_{C_3}]_S=\frac{A_d^2}{2\epsilon^2(1+\nu)}\left\{1+\frac{\epsilon}{2}\left[1+\ln\frac{1+\nu}{1+\mu}-\sigma\ln\frac{1+\sigma}{\sigma}\right]+\epsilon\frac{b}{a-b}-\epsilon\frac{a^2\ln a+b^2\ln b-2ab\ln b}{(a-b)^2}\right\}, \tag{A33}$$

$$[I_{C_5}]_S=\frac{A_d^2}{2\epsilon^2(1+\nu)}\left\{1+\frac{\epsilon}{2}\left[1+\ln\frac{1+\nu}{\mu+\nu}+\frac{\sigma}{\nu^2}\ln\frac{\sigma}{(1+\nu)(\mu+\nu)}\right]-\epsilon\frac{a\ln a-b\ln b}{a-b}\right\}. \tag{A34}$$

APPENDIX B: DEFINITION OF THE RENORMALIZATION FACTORS

The renormalization of the Ginzburg-Landau-Wilson functional (7) is well known within different renormalization schemes [20,22,34,35]. The extended static functional determined by Eq. (6) has been considered in detail in [13] using the normalization condition approach and in [36] within the minimal subtraction procedure. The justification of several relations between the static Z factors mentioned below can be found in [36,37].

For the order parameter $\vec{\psi}$ we introduce the renormalization factor

$$\vec{\psi}_0=Z_\psi^{1/2}\vec{\psi},\quad \vec{\psi}_0^\dagger=Z_\psi^{1/2}\vec{\psi}^\dagger, \tag{B1}$$

where Z_ψ is a real quantity. The renormalization of the fourth-order coupling u appearing in Eq. (7) is defined as usual:

$$\mathring{u}=\kappa Z_\psi^{-2}Z_u u A_d^{-1}. \tag{B2}$$

κ represents a free wave number scale. To complete the renormalization of Eq. (7) a Z factor

$$\frac{1}{2}|\psi_0|^2=Z_{\psi^2}\frac{1}{2}|\psi|^2 \tag{B3}$$

is necessary to renormalize correlation functions containing $1/2|\psi|^2$ insertions. At least the correlation function $\langle 1/2|\psi_0|^2 1/2|\psi_0|^2\rangle_c$ (the subscript c denotes the cumulant), which represents the specific heat within the model, needs an additive renormalization A_{ψ^2}.

Concerning the Ginzburg-Landau-Wilson model we want to remark that the usage of the minimal subtraction approach as a renormalization scheme makes it necessary to introduce a renormalization for the parameter r in the form of

$$\mathring{r}=Z_\psi^{-1}Z_r r. \tag{B4}$$

This renormalization is connected to the renormalization of the $1/2|\psi|^2$ insertions by the relation $Z_{\psi^2}=Z_\psi^{-1}Z_r$. As a consequence no necessity is given to consider correlation functions containing $1/2|\psi|^2$ insertions explicitly within the minimal subtraction approach apart from $\langle 1/2|\psi_0|^2 1/2|\psi_0|^2\rangle_c$ itself.

The additional quantities in the extended static functional (6) require the introduction of further renormalization factors. The secondary density m and the coupling parameter γ between order parameter and secondary density, which guarantees a nontrivial static critical behavior of the thermodynamic derivatives, will be renormalized analogously to Eq. (B2) by

$$a_m^{1/2}m_0=Z_m m, \tag{B5}$$

$$a_m^{-1/2}\mathring{\gamma}_m=\kappa^{\epsilon/2}Z_\psi^{-1}Z_m^{-1}Z_\gamma\gamma A_d^{-1/2}. \tag{B6}$$

Note that we have introduced the Z factor Z_m instead of $Z_m^{1/2}$ contrary to most of the definitions in the literature. Our definition is more convenient when one wants to maintain consistency with the definitions necessary in model F' (describing the critical dynamics at the superfluid transition in ^{3}He-^{4}He mixtures [16]) where a matrix Z_m had to be introduced.

Since the static functional of model C^* is a Gaussian extension of the Ginzburg-Landau-Wilson model, no new independent renormalization factors are necessary. Thus relations between the Z factors of the Ginzburg-Landau-Wilson model and the model C^* parameters arise. First the renormalization factor of the coupling γ is determined by

$$Z_\gamma=Z_m^2 Z_\psi Z_{\psi^2}, \tag{B7}$$

leading with Eq. (B6) to

$$a_m^{-1/2}\mathring{\gamma}_m=\kappa^{\epsilon/2}Z_{\psi^2}Z_m\gamma A_d^{-1/2}. \tag{B8}$$

Second, the renormalization factor Z_m of the secondary density is determined by the additive renormalization $A_{\psi^2}(u)$ of the specific heat in the Ginzburg-Landau-Wilson model. This gives

$$Z_m^{-2}(u,\gamma)=1+\gamma^2 A_{\psi^2}(u). \tag{B9}$$

In the dynamic functional auxiliary fields $\tilde{\vec{\psi}}_0$ and $\tilde{m}_0$ are introduced, which renormalize like

$$\tilde{\vec{\psi}}_0=Z_{\tilde{\psi}}^{1/2}\tilde{\vec{\psi}},\quad \tilde{\vec{\psi}}_0^\dagger=Z_{\tilde{\psi}^\dagger}^{1/2}\tilde{\vec{\psi}}^\dagger. \tag{B10}$$

The renormalized auxiliary density $\tilde{\vec{\psi}}^\dagger$ is complex conjugated to $\tilde{\vec{\psi}}$ quite analogous to the corresponding unrenormal-

ized densities; thus, we have $Z_{\tilde{\psi}^\dagger}=Z_{\tilde{\psi}}^\dagger$. The secondary density is conserved and therefore no new renormalization factor is needed for the corresponding auxiliary density. It simply renormalizes:

$$a_m^{-1/2}\tilde{m}_0=Z_m^{-1}\tilde{m}. \tag{B11}$$

At least the kinetic coefficients renormalize as

$$\mathring{\Gamma}=Z_\Gamma\Gamma, \quad a_m\mathring{\lambda}_m=Z_\lambda\lambda. \tag{B12}$$

The Z factors in the above equations contain static contributions which may be separated:

$$Z_\Gamma=Z_\psi^{1/2}Z_{\tilde{\psi}^\dagger}^{-1/2}Z_\Gamma^{(d)}, \quad Z_\lambda=Z_m^2Z_\lambda^{(d)}. \tag{B13}$$

The absence of any mode coupling in model C^* leads to trivial renormalization factors of the dynamic parts of the kinetic coefficients:

$$Z_\Gamma^{(d)}=1, \quad Z_\lambda^{(d)}=1. \tag{B14}$$

Thus Eq. (B13) reduces in model C^* to

$$Z_\Gamma=Z_\psi^{1/2}Z_{\tilde{\psi}^\dagger}^{-1/2}, \quad Z_\lambda=Z_m^2. \tag{B15}$$

Only the renormalization factor $Z_{\tilde{\psi}^\dagger}^{-1/2}$ has to be determined from dynamic perturbation theory.

[1] B. I. Halperin, P. C. Hohenberg, and Shang-keng Ma, Phys. Rev. Lett. **29**, 1548 (1972) (model *A*).

[2] B. I. Halperin, P. C. Hohenberg, and Shang-keng Ma, Phys. Rev. B **10**, 139 (1974) (model *C*).

[3] K. Oerding and H. K. Janssen, J. Phys. A **26**, 3369 (1993).

[4] W. Koch and V. Dohm, Phys. Rev. E **58**, R1179 (1998).

[5] G. Grinstein, Shang-keng Ma, and G. F. Mazenko, Phys. Rev. B **15**, 258 (1977).

[6] P. Calabrese and A. Gambassi, Phys. Rev. E **67**, 036111 (2003).

[7] V. I. Gorentsveig, P. Fratzl, and J. L. Lebowitz, Phys. Rev. B **55**, 2912 (1997).

[8] K. Binder, W. Kinzel, and D. P. Landau, Surf. Sci. **112**, 232 (1982).

[9] H. Tanaka, J. Phys.: Condens. Matter **11**, L159 (1999).

[10] E. D. Siggia and D. R. Nelson, Phys. Rev. B **15**, 1427 (1977).

[11] B. Berdnikov and K. Rajagopal, Phys. Rev. D **61**, 105017 (2000).

[12] S. Borsányi, A. Patkós, D. Sexty, and Zs. Szép, Phys. Rev. D **64**, 125011 (2001).

[13] E. Brezin and C. De Dominicis, Phys. Rev. B **12**, 4954 (1975).

[14] K. K. Murata, Phys. Rev. B **13**, 2028 (1976).

[15] B. I. Halperin, P. C. Hohenberg, and Shang-keng Ma, Phys. Rev. B **13**, 4119 (1976).

[16] R. Folk and G. Moser, Phys. Rev. Lett. **89**, 125301 (2002).

[17] R. Folk and G. Moser, Acta Phys. Slov. **52**, 285 (2002).

[18] R. Folk and G. Moser, Phys. Rev. Lett. **91**, 030601 (2003).

[19] V. Dohm, Phys. Rev. B **44**, 2697 (1991).

[20] G. Parisi, J. Stat. Phys. **23**, 49 (1980).

[21] D. J. Amit, *Field Theory the Renormalization Group and Critical Phenomena*, 2nd ed. (World Scientific, Singapore, 1984).

[22] R. Schloms and V. Dohm, Nucl. Phys. B **328**, 639 (1989).

[23] Although the definitions of the ζ functions (11) for the dynamical parameters and the renormalization factors (B12) are different, the explicit expressions of the ζ functions are in agreement with [19].

[24] After finishing our calculations we have been informed by V. Dohm of unpublished calculations by K. Oerding. His results for the dynamical ζ functions agree with ours.

[25] We use, however, also in this case the ϵ-expanded fixed-point values of the static couplings. The two-loop β function for u has no real solution and one had to use the Borel-summed β function, which is not known for general n.

[26] A. Pelissetto and E. Vicari, Phys. Rep. **368**, 549 (2002).

[27] Yu. Holovatch, M. Dudka, and T. Yavors'kii, J. Phys. Stud. **5**, 233 (2001).

[28] The parameter c has been calculated in three-loop order in [13] and corrected by Antonov and Vasil'ev [29]. The reason why the result of [29] is more reliable is the fact that c would be negative for $d<3.70$ ($\epsilon>0.296$) in [13], whereas this happens only for $d<1.35$ ($\epsilon>2.65$) in [29].

[29] N. V. Antonov and A. N. Vasil'ev, Theor. Math. Phys. **60**, 671 (1984).

[30] J. Zinn-Justin, *Quantum Field Theory and Critical Phenomena* (Clarendon Press, Oxford, 1997).

[31] Note that in [18] the dynamical critical exponent z for model A has been missprinted due to an erroneous minus sign before $c\,\eta$.

[32] In [13] a renormalization with normalization conditions has been used. Therefore, in the comparison with our renormalization scheme using the minimal subtraction scheme in the ζ functions of [13] ϵ has to be set to zero.

[33] R. Bausch, H. K. Janssen, and H. Wagner, Z. Phys. B **24**, 113 (1976).

[34] E. Brezin, J. C. Le Guillou, and J. Zinn-Justin, in *Phase Transitions and Critical Phenomena*, edited by C. Domb and M. S. Green (Academic, New York, 1976), Vol. 4.

[35] I. D. Lawrie, J. Phys. A **9**, 961 (1976).

[36] V. Dohm, Z. Phys. B: Condens. Matter **60**, 61 (1985).

[37] E. Eisenriegler and B. Schaub, Z. Phys. B: Condens. Matter **39**, 65 (1980).

[38] D. Stauffer, Int. J. Mod. Phys. C **8**, 1263 (1997); P. Sen, S. Dasgupta, and D. Stauffer, Eur. Phys. J. B **1**, 107 (1998); B. Zheng and H. J. Luo, Phys. Rev. E **63**, 066130 (2001).